EUROPEAN FORUM for RECIPROCATING COMPRESSORS

1st EFRC - Conference

The Recip - a State of the Art Compressor

Der Kolbenkompressor - eine zeitgemäße Arbeitsmaschine

4. - 5. November 1999, Dresden, Germany

Inhalt / Contents

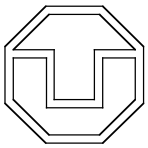

Wear Estimate of the Sealing Ring – Effect on the Operating Parameters of a Reciprocating Compressor

by:
Hans-Joachim Kleinert and Gotthard Will
Professorial Chair for Pumps, Compressors and Apparatus
Dresden University of Technology
Germany

The Recip – a State of the Art Compressor
4th to 5th November 1999, Dresden

Abstract:

Knowing the operating parameters of the compressor, the structural design of the piston seal and the properties of the ring material we are able to carry out a proximate wear calculation of dry-running sealing rings. The calculation is based on the wear model by KRIEGEL and the sealing chamber pressure distribution by EWEIS/BECKMANN. The pre-calculation of the ring wear and the leakage losses result in recommendations for the structural design of the piston seal as well as in the selection of the machine parameters for dry-running.
Fuzzy classification is applied to investigate the reflection of piston ring leakiness in the stage pressures and temperatures.

1 Introduction

Long maintenance-free running times are required to guarantee the economic operation of reciprocating compressors. The admissible maintenance interval for dry-running reciprocating compressors is most of all limited by the necessity to change the ring. Therefore, the mechanisms and influence quantities of the ring wear of dry-running reciprocating compressors have frequently been the subject of numerous research projects and publications[1,2,3].

This paper will give an overview of the quantitative interrelations of the origination and effects of wear, which supplement the construction rules established by Kleinert[4] for dry-running reciprocating compressors. These additional rules can help producers and operators make decisions. The interrelations have been derived with calculation programmes that have been worked out within study projects at the Professorial Chair for Pumps, Compressors and Apparatus at Dresden University of Technology.

2 Pre-Calculation of the Ring Wear and the Leakage Flows – Preconditions

In accord with the wear model by Kriegel[5] the radial ring wear Δr of dry-running piston rings is proportional to the wear way L and the mean radial contact pressure p.

$$\Delta r = K \cdot L \cdot p \tag{1}$$

The proportional action factor K is denoted as wear factor which primarily depends on the material and is at the same time influenced by the piston speed, the temperature and roughness of the running surface as well as the humidity of the material conveyed, however. According to [5] it is possible to predict the wear factor by systematic investigations in a wear machine, which collect the interrelations mentioned above. For the calculations given later in this paper the investigation results have been described as follows:

$$K = K_0 \cdot \lambda_t \cdot \lambda_v \cdot \lambda_R \cdot \lambda_\varphi \tag{2}$$

with K_0 being the material-conditioned rate of wear under reference conditions and λ_t, λ_v, λ_R, λ_ϕ being the influence factors of the temperature, running speed, roughness and the temperature of dew point, which are defined as follows

$$\lambda_t = 0.74\left(t/t_b\right)^2 - 0.44\left(t/t_b\right) + 0.70 \tag{1}$$

$$\lambda_v = 0.70\left(v/v_b\right)^2 + 0.30 \tag{2}$$

$$\lambda_R = 0.41\left(R/R_b\right)^2 - 0.58\left(R/R_b\right) + 1.17 \tag{3}$$

$$\lambda_\varphi = \begin{cases} 0.043\left(\Phi/\Phi_b\right)^2 + 0.159\left(\Phi/\Phi_b\right) + 0.171 \\ 1 \qquad \text{für } \Phi \geq -30°C \end{cases} \tag{4}$$

with the reference values t_b=100°C, v_b=2.85m/s, R_b=1µm and Φ_b=10°C.

Further investigations into the wear behaviour of dry-running materials have been carried out by Tomschi[6]. New data have been accessed on the relationship between gas atmosphere, ring material and slipway structure and the Kriegel wear model has principally been confirmed.

If we start from the facts that the radial ring wear Δr, which is admissible for reasons of strength, is proportional to the piston diameter d and that the wear factor K grows approximately proportionally to the mean piston speed c_m, we get the following proportionality for the ring service life τ_L with $L = c_m \cdot \tau_L$.

$$\tau_L \sim d/\left(p \cdot c_m^{\,2}\right) \tag{7}$$

The chamber pressure distribution, which depends on the status process in the neighbouring working areas, is an essential feature to determine the time-variable radial contact pressure p of the piston rings.

Eweis[7] was the first to calculate the time march of the chamber pressure. Beckmann[8] proved that calculation and measurement sufficiently correspond to each other for a dry-running reciprocating compressor. A computing programme has been prepared and developed within the study projects[9,10] which allows the one-step determination of the pressure and temperature data in the chambers as well as the ring wear for given packing ring designs and operating parameters.

The chamber pressure calculation implies the time-variable mass flows that also occur between the working area and the individual chambers. Thus integral statements can be made with regard to the influence of the leakage flow on the mass as well as to the energy balance in the working area. Since the outlet and inlet flows towards the working area take place at the time-variable specific working capacity of the working fluid and since they may even be balanced e.g. for double-acting pistons during one cycle, we advocate the introduction of a tightness efficiency instead of a tightness coefficient, which assesses the leak flow only. The tightness coefficient relates the working capacity loss ΔW connected with the leak flow m_l to the interior work W according to eq. (4):

$$\eta_d = W/\left(W + \Delta W\right) \quad \text{with} \quad \Delta W = \int_{\tau=0}^{1/n} e\,\dot{m}_l\,d\tau \tag{8}$$

Beckmann's[8] model tests show that the percentage of the leak flow through the open joint amounts to about 80 to 90 % for new rings with butt joints. Naturally, the leak flow through the open joint increases with the operation time progressing, while the leak flows through the radial and axial gaps remain constant, approximately. For this reason, the calculation is simplified and refers to the leak flow through the open joint of the ring only.

3 Influencing the Ring Wear and the Tightness Efficiency During the Compressor Design Phase

3.1 Influence of the Seal Design

If the stage pressure and dimensions were fixed during the machine planning stage and if for the ring a material is used that is most suitable for the material to be conveyed, the only way to influence wear during the design phase is via the mean radial contact pressure p. It is

therefore likely to assume that the number of sealing rings primarily determines the contact pressure. The latter may quite as well be influenced by the storage effect of the intermediate chambers.

Figure 1 shows the calculated mean radial contact pressure of the individual rings with reference to the stage pressure increase for different ring numbers for the example of a single-acting and a double-acting compressor stage with the pressure ratio π=3. Figure 1 demonstrates that the contact pressure of the first piston ring for the single-acting piston and of the two external piston rings for the double-acting piston amounts to about 16 to 19 % of the maximum pressure differential above the piston and is nearly independent of the number of rings. If the chamber volumes are increased the external ring load grows slightly. Increasing ring wear is of similar effect. The number of rings is of clearly positive effect on the leak flow and the tightness efficiency.

Figure 2 shows the decrease of the tightness efficiency as a result of the piston ring wear plotted over time for the same conditions as in Fig. 1. For a radial ring wear of 30 % and a double-acting piston a decrease of the tightness coefficient from 99 % to 95 % for 8 rings and to 89 % for 4 rings, respectively is to be expected.

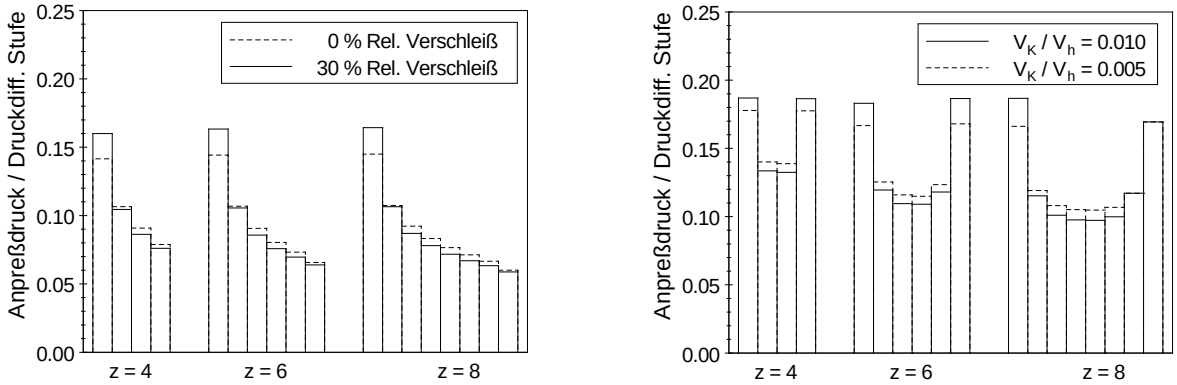

Fig. 1: Mean radial contact pressure of the piston rings for different ring numbers
a) single-acting *b) double-acting piston*

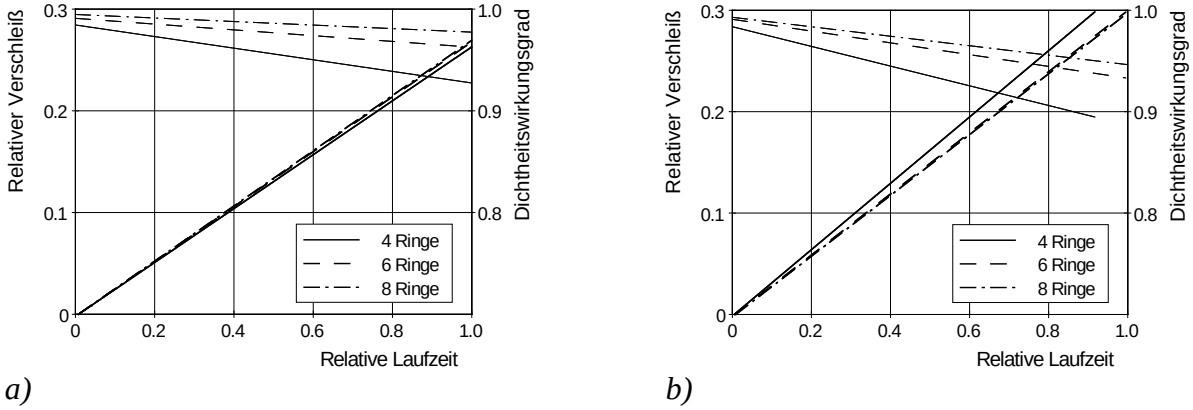

Fig. 2: Time history of the ring wear and the tightness efficiency for different ring numbers
a) single-acting *b) double-acting piston*

If - by carrying out the piston rings as captive rings - the service life of a sealing ring is limited until the admissible wear is obtained, the service life of the overall seal can be extended. Principally, the number of effective piston rings is thus gradually reduced, while the service life of the piston rings, that act as the most external sealing ring one after the other, decreases owing to the already existing wear. On the other hand, the tightness efficiency is progressively decreasing. Fig. 3 shows the results of a relevant recalculation.

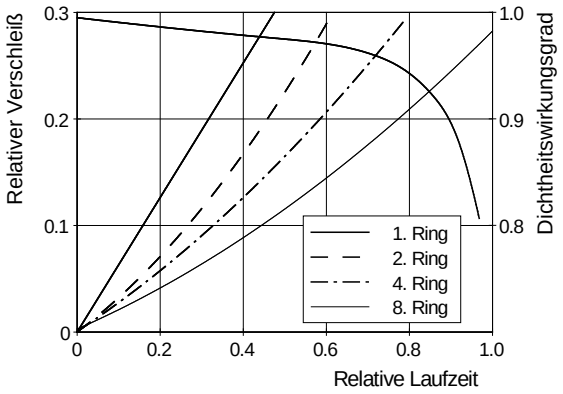

Fig. 3: Time history of the ring wear and the tightness efficiency for a piston seal with captive rings

Proportionality (7) reveals that a fast ring wear can hardly be avoided in high pressure stages. Except for the development of ring materials with a relatively low wear factor, the application limits of dry-running have been shifted by reducing the pressure differential by means of a pre-connected labyrinth-sealing[11]. The pressure-reducing effect of the labyrinth is felt only when a certain leakage is obtained, i. e., it gradually reduces the ring wear, which is very fast in the beginning.

In order to quantify this relation we can start from the equation for mass flow by labyrinths[12]

$$\dot{m}_l = K_L \, \pi \, d \, \delta \sqrt{\frac{p_D{}^2 - p_z{}^2}{z \, p_D / \rho_D}} \tag{9}$$

with p_z is the pressure after z labyrinth chambers, K_L is a constant describing the labyrinth design and δ is the labyrinth gap width. On the other hand, this mass flow can be related to the piston displacement stream and the tightness coefficient λ_d of the stage.

$$\dot{m}_l = (1-\lambda_d)\rho_S \, \dot{V} = (1-\lambda_d)\rho_D \left(\frac{p_S}{p_D}\right)^{1/\kappa} \frac{\pi}{4} d^2 \frac{c_m}{2} \lambda_h \tag{10}$$

Equating the right sides and solving the equation for the interesting pressure ratio p_z/p_D we get

$$p_z / p_D = \sqrt{1 - K_K K_B (1 - \lambda_d)^2} \tag{5}$$

$$\text{mit} \quad K_K = \frac{z}{64 K_L^{\,2}} \left(\frac{d}{\delta} \right)^2 \tag{6}$$

$$K_B = \left(\frac{p_S}{p_D} \right)^{2/\kappa} \frac{c_m^{\,2}}{R T_D} \lambda_h^{\,2} \tag{7}$$

The constants K_K and K_B describe the labyrinth design conditions and the stage operating parameters, respectively. Fig. 4 offers a help to decide which labyrinth design is necessary for the actual case, e. g. to reduce the pressure differential above the piston ring seal by 50 %. Fig.5 shows the wear and tightness characteristics for a combined labyrinth-piston ring seal over time.

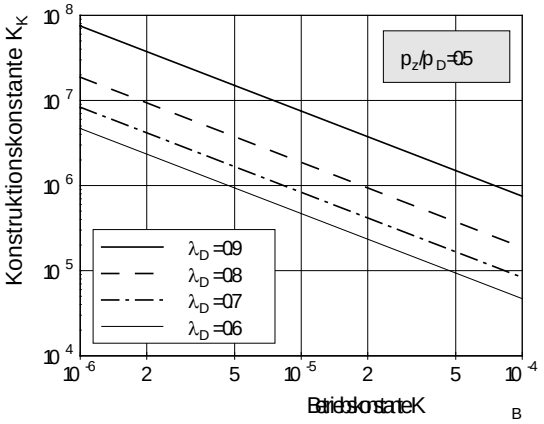

Fig. 4: Effect of design and operating parameters on the functioning of a combined labyrinth-piston ring seal

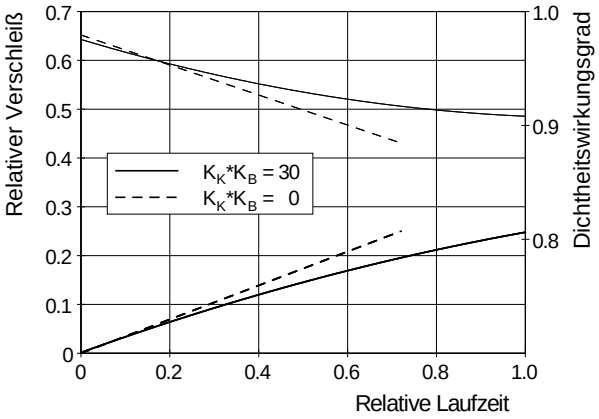

Fig. 5: Wear and tightness curves over time for a combined labyrinth-piston ring seal

The volume flow through the open joint has so far been calculated with the drag coefficient 1, which corresponds to complete dissipation of the kinetic energy for even velocity distribution in the narrowest cross section of the joint. For a better comprehension of the flow in the open joint and to find out about the drag of different joint forms with the wear growing, the gap flow has been examined for typical gap forms and dimensions using the

Navier-Stokes code TASCFLOW. Fig. 6 and 7 show the velocity distributions for the straight and the interleaved joint in the narrowest cross section of the open joint. The related kinetic energy is greater by the factor 1.7 and 2.9, respectively, compared with the kinetic energy ρ^2 /2 that is necessary for even orthogonal flows through the cross section, which results in equal drag coefficients for subsequent complete dissipation.

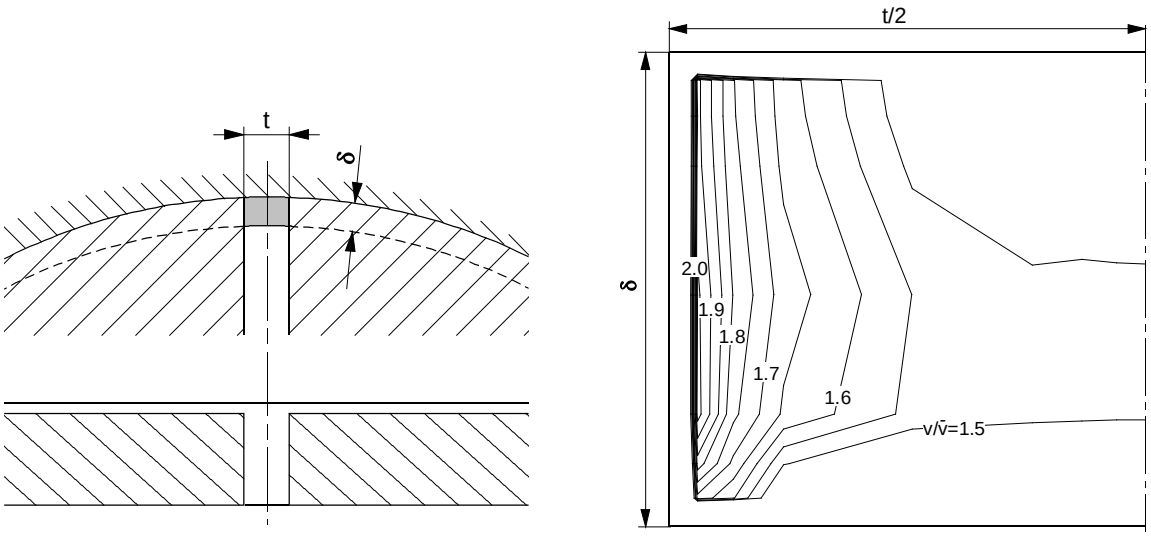

a) *b)*

Fig. 6: Flow in the straight open joint
a) given geometry
b) calculated velocity distribution in the narrowest cross section

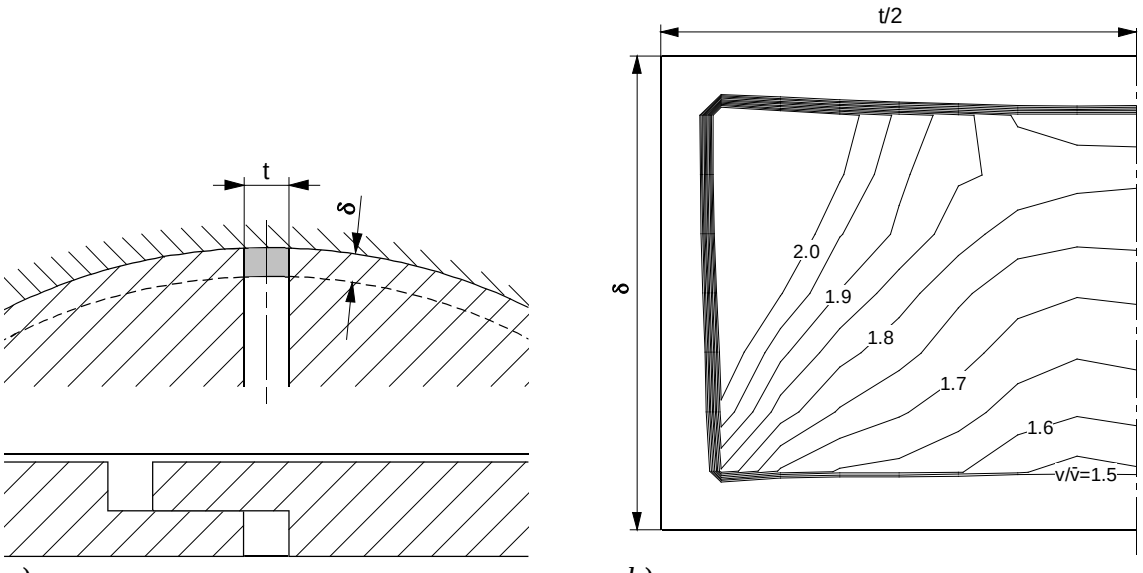

a) *b)*

Fig. 7: Flow in the straight interleaved open joint
a) given geometry
b) calculated velocity distribution in the narrowest cross section

3.2 Influence During Planning Stage

When the most essential parameters are being selected during the machine planning stage attention has to be paid to the relations for the ring wear (1) and the service life (7). Since the mean contact pressure p of the external rings related to the maximum pressure differential – see paragraph 3.1 – can hardly be influenced by the seal design for a given pressure ratio, the service life of the piston rings can principally be extended only by reducing the stage pressure ratio or the mean piston speed.

As a first step, we have therefore examined the influence of the pressure ratio of a double-acting stage on the service life of the piston rings and the tightness efficiency for the example discussed in 3.1. As expected, the contact pressure together with the wear increase linearly with π (Fig. 8).

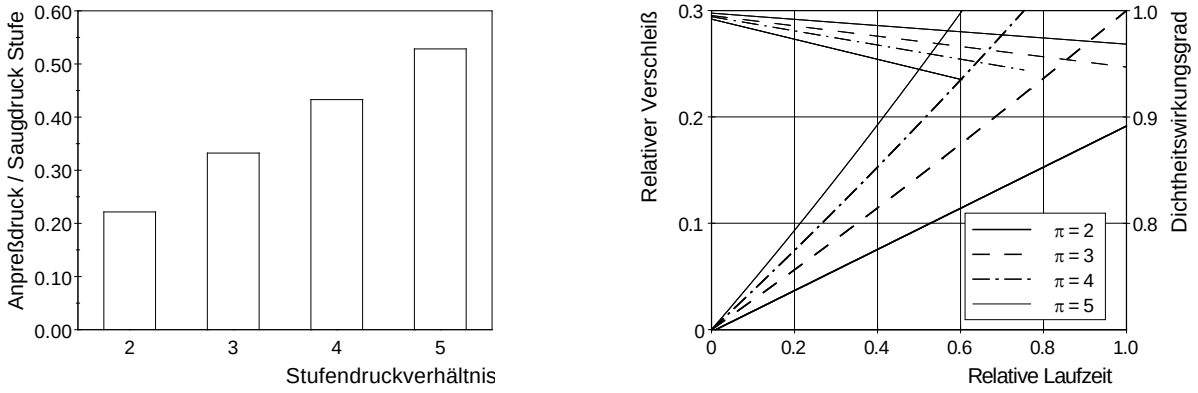

Fig. 8: Wear and tightness curves over time as a function of the pressure ratio

Further calculations have been carried out with the secondary condition of a constant piston displacement stream to find out to which extent proportionality (7), which is derived for simplified assumptions, is valid.

First, stroke and speed have been varied for an invariable diameter such that the mean piston speed remained constant. It is clear that with increasing s/d, i. e. with decreasing speed the contact pressure of the external rings decreases slightly, which reduces the wear (Fig. 9). The constant tightness efficiency demonstrates that the larger joint area is compensated by the shorter period of time with regard to the leak flow.

Afterwards, the mean piston speed has been increased for constant s/d. This results in a slight contact pressure increase and a decrease of the service life, which is more than quadric (Fig. 10).

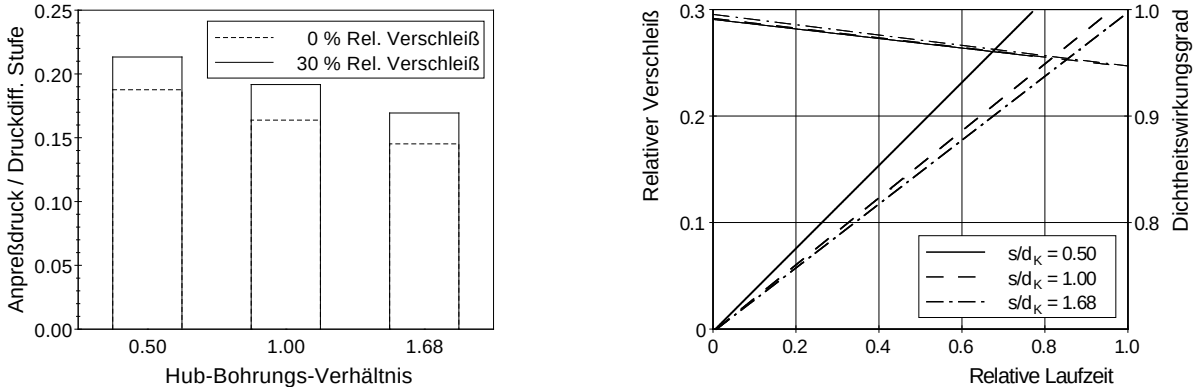

Fig. 9: Wear and tightness curves over time as a function of the stroke drilling relation

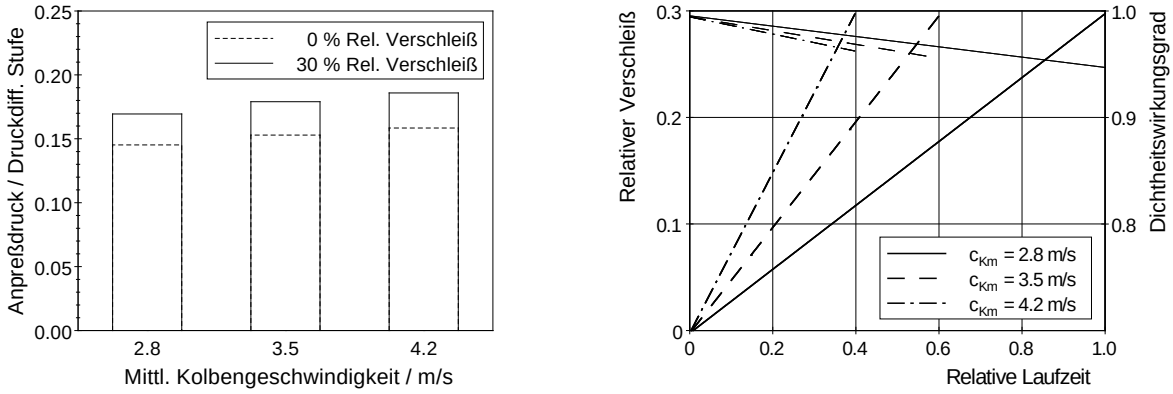

Fig. 10: Wear and tightness curves over time as a function of the mean piston velocity

4 Effects and diagnosis of wear

The pre-calculation of the ring wear for known design and operating parameters provides a first help for compressor makers to determine the admissible maintenance interval. Criteria for the calculation are the lower deviation of the ring strength and the decrease of the tightness efficiency. The question which minimum tightness efficiency can be accepted has to be answered on an economic background. The sum of overhead costs should be minimised.

If the compressor is operated with the ring wear increasing further effects have to be considered, however. Inner leakiness, e.g. may contribute to a higher outlet temperature of the stage. Moreover, the intermediate pressures shift in the individual stages of multistage compressors with different inner leakiness. These effects should be paid attention to both in the planning stage and when the compressor is in operation.

Ideally, a process compressor is constantly monitored by a complex diagnosis system. In addition to a vibration analysis, which is mainly carried out to detect damages in the driving mechanism (Triebwerk), the pressures and temperatures at the stage inlets and outlets are checked. It is also recommended to consistently measure the compressor's flow rate and the shaft power. Moreover, in particular cases, the pressure curve in the working areas is determined and interpreted by indicating.

Changes due to worn tight elements and valves may be detected by trend analyses. It is relatively complicated to draw conclusions in terms of the seize and location of excessive wear. Fuzzy logic is frequently applied for this purpose, namely the method of fuzzy classification. This method is based on a classifier which compares all available and useful measured data in the form of a feature set with feature sets for defined damage classes. The fuzzy classification method provides probabilities with which the actual feature set my be assigned to a specific damage class. The fuzzy classification requires a sufficient number of characteristic feature sets as a pre-condition for the defined damage classes to „train" the classifier.

The generation of such feature sets by operating the machine with simulated damages at all wearing parts - in particular for different stages of damage extent and any combinations - is practically not possible for larger process compressors of individual make whose test run takes place directly in the plant. Hence this huge amount of feature sets may only be provided in a theoretical way. In the study project[13] an attempt was made to generate the feature sets of

damage classes implying leakiness at the valves, the piston rings and the piston shaft packings of all stages by means of a simulation calculation for all of the machine with the leakiness given for a four-stage process compressor.

Some of the project[13] results will be presented in the following. They refer to the detection of growing piston ring leakiness using the double-acting second stage of the compressor as an example. In a double-acting stage the gas flows through the leaky piston rings with a higher temperature from the just compressing working area into the suction area thus increasing the initial temperature of the compression process there. As a result of leakiness the stage pressure ratio decreases so that the outlet temperature remains nearly constant, however (Fig. 11). A clear effect of the growing leakiness can only be detected if pressure ratio and temperature ratio of the stage are compared (Fig. 12).

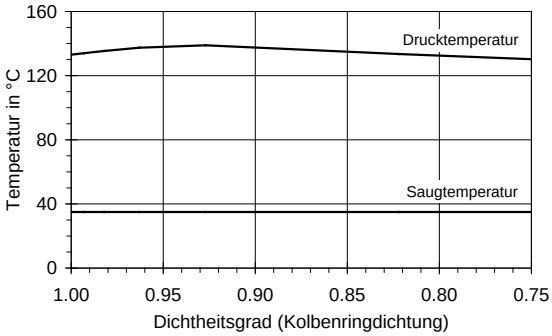

Fig. 11: Pressure temperature and suction temperature of the second stage for increasing piston ring leakiness

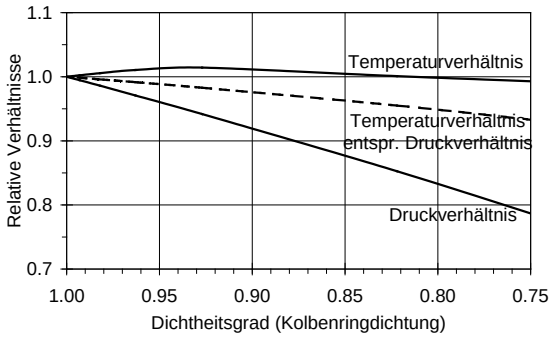

Fig. 12: Pressure ratio and temperature ratio of the second stage for increasing piston ring leakiness

Unfortunately, the leakiness effects at both valves are similar so that most often only the diagnosis of growing inner leakiness as a result of both causes is possible. In the case of the fourth stage of the compressor, in which only inner leakiness may occur, a certain differentiation between ring leakiness and valve leakiness may be successful if two suitable feature sets are selected (Fig. 13). Here, the abscissa is the standardised pressure ratio of the third stage, while the standardised product of volume flow and pressure ratio of the fourth stage is used as the ordinate.

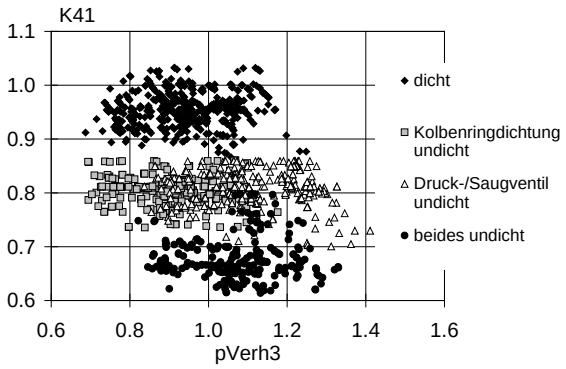

Fig. 13: Differentiation between various leakinesses at the fourth stage

5 Summary

The calculation method presented provides information about the effect of various design parameters on the ring wear of dry-running reciprocating compressors.

In a first approximation the service life of the piston rings is inversely proportional to the stage pressure differential and to the squared mean piston speed as well. A larger number of rings reduces only the leak flow with the wear rate remaining the same. An extension of service life times may be obtained by special piston seal designs for given ring materials and pressure differentials.

The accuracy of service life forecasts of piston rings for actual operating parameters is limited by the accuracy of the model assumptions and the empirical relations as well. If the number of measured data on the piston ring wear within known operating parameters is sufficiently large, their analysis might contribute to the validation and improvement of the calculation procedure presented.

The diagnosis of excessive piston ring leakiness carried out by means of pressure and temperature measurements between the stages is difficult and remains relatively fuzzy even if suitable characteristic numbers are applied, since valve leakiness produces similar effects.

References

[1] Notaro, J.: Trockenlaufkolbenringe für die Anwendung bei hohem Druck. Lubrication Engineering (1966), S. 104 – 108

[2] Davydov, K.S.: Die Untersuchung des Arbeitsprozeßes von Verdichtern mit hohem Druck und nichtmetallischer Kolbenabdichtung ohne Schmierung. Trudy LPI Nr. 310 (1969), S. 200 – 203

[3] Bartmann, L.: Beitrag zur Bestimmung der Leckverluste im Arbeitszylinder eines Kolbenkompressors. Doctoral Thesis TH Karlsruhe, 1968

[4] Kleinert, H. J.: Auslegungs- und Konstruktionsprobleme bei Trockenlauf-Hubkolbenkompressoren und deren Gestaltungsmerkmale. In Proceedings der Fachtagung Entwicklung und Betrieb von Kolbenverdichtern. TU Dresden 1997

[5] Kriegel, G.: Beitarg zur Berechnung des Radialverschleißes von Trockenlaufkolbenringen. Doctoral Thesis TU Dresden, 1977

[6] Tomschi, U.: Verschleißverhalten von Trockenlaufwerkstoffen für Abdichtelemente in Kolbenkompressoren. Doctoral Thesis Universität Erlangen-Nürnberg, 1995

[7] Eweis, W. : Reibungs- und Undichtheitsverluste an Kolbenringen. VDI-Forschungsheft 371, VDI-Verlag Berlin 1935

[8] Beckmann, W.: Ermittlung von Einflußfaktoren auf das Betriebsverhalten trockenlaufender Kolbenringdichtungen. Doctoral Thesis TU Dresden, 1985

[9] Scholz, A.: Erarbeitung eines FORTRAN-Programms zur Berechnung der Druckverteilung in einer Kolbenringdichtung. Assigned Paper TU Dresden, 1992

[10]Braun, M.: Simulation des Betriebsverhaltens einer Kolbenringdichtung. Diploma Paper TU Dresden, 1993

[11]Nickol, J.: Verschleißuntersuchungen von trockenlaufenden Abdichtelementen bei Kolbenkompressoren. In Proceedings der Fachtagung Entwicklung und Betrieb von Kolbenverdichtern. TU Dresden 1994

[12]Taschenbuch Maschinenbau Band 5, Verlag Technik Berlin 1989

[13]Leupold, P.: Aufbau und Erprobung von FCT-Klassifikatoren. Diploma Paper TU Dresden, 1996

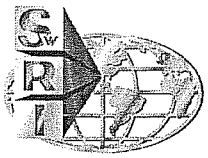

Foundation Health and Compressor Reliability

by:

Harrell, J. P.

Smalley, A. J.

Mechanical & Fluids Engineering Department

Southwest Research Institute

San Antonio, Texas

U.S.A.

Session 4

The Recip - a State of the Art Compressor
4. – 5. November 1999, Dresden

Abstract:

Large reciprocating compressors interact with their foundations in critical ways, and many mechanisms that decrease compressor reliability result from foundation and mounting problems. A multi-year research effort has explored the interactions between the compressor and its foundation, leading to important insights and guidelines for maintaining reliability. This paper reviews and summarizes the research and its results. It addresses analysis of compressor loads and shaking forces, foundation design and concrete cracking, anchor bolt practice, behavior of chocks and epoxy grouts, effects of oil on foundations and chocks, bearing alignment issues, cylinder alignment issues, and crankshaft health issues.

1 Introduction

Large reciprocating compressors depend on their foundation for structural integrity. As this paper will show, their frames alone have insufficient rigidity to support internally generated forces, and the foundation must become an integral part of the machine. Recognizing this should influence the methods used to design and repair the foundation, and to attach the compressor to its foundation. When the foundation and compressor body do not act together due to an inadequate or deteriorated foundation, the most obvious symptom is high horizontal vibration with bending of the frame and relative motion across the interface between foundation and compressor. Figure 1 illustrates this symptom. Even new installations can exhibit similar characteristics if inadequately designed or installed. A long series of investigations, supported by PRC *International* (PRC*I*)[1] and by the Gas Machinery Research Council (GMRC), has posed and answered many questions critical to the design of effective, robust, long lived installations[2,3]. The research has also developed some working level condition monitoring tools and criteria though the prognostic area still presents a challenge.

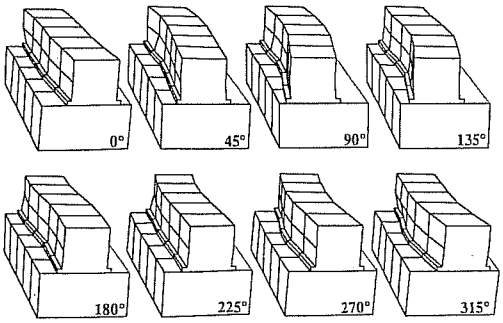

Figure 1. Deflected Shapes of a Compressor Frame for Each 45 Degrees of Crankshaft Rotation

This paper presents results of this research program emphasizing the essential knowledge which has been generated, including previously unavailable data, recently developed, on mechanical characteristics of compressor mounts. Most of the data presented can be accessed through the Internet, as defined in the reference list.

2 The Consequences of Deteriorated Mounts and Foundations

Figure 2 shows two crankshafts which failed in bending. This failure commonly occurs across one of the webs joining crank pin to main bearing as a result of misalignment. Figure 3 contrasts this characteristic with a torsional failure and its classic 45-degree fracture line. A survey undertaken in 1993 to profile crankshaft failures in large reciprocating compressors showed that deteriorated or sagging foundations represented the predominant cause of crankshaft failures, accounting for almost half of the attributed causes. Figure 4 presents this data in bar graph form[4].

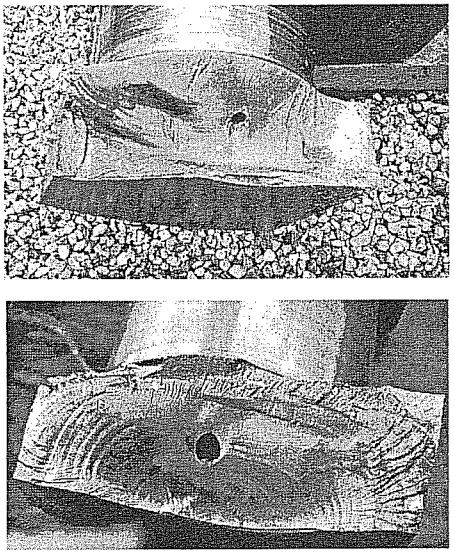

Figure 2. Crankshaft Bending Failure Examples

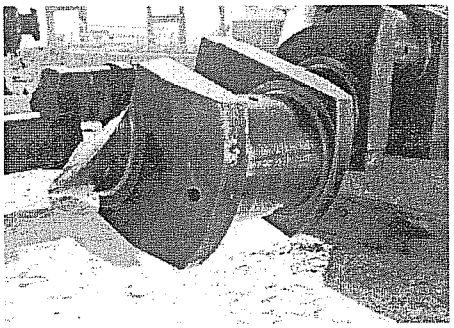

Figure 3. Torsional Fracture of Crankshaft (Note 45° Fracture Line)

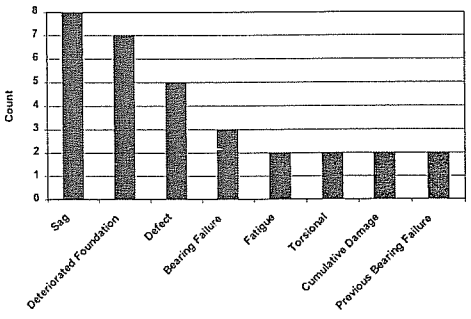

Figure 4. Count of Primary and Secondary Causes Associated with Fractured Shafts

Figure 5 illustrates the web deflection method – a very widely applied measure of crankshaft alignment condition. Offset of main bearings from a straight line bends the crankshaft and changes the separation of crank web faces as the unit is barred over. This same bending imposes one per rev stress reversals on top of normal operating stresses. The widely applied Caldwell criterion limits web deflections to the stroke multiplied by 1.8 x 10^{-4}. Some operators use a fixed limit – typically 50 microns, though ranging from 25 to 100 microns. Figure 6 shows a crankshaft ready for laboratory testing. Figure 7 shows close agreement between predictions and measurement of web deflection as a function of crankshaft angle relative to the bending load vector[5]. The testing showed for two crankshafts (a Clark HBA and Cooper GMV), a range of stress from 17.6 to 21.3 MPa when at the Caldwell limit. Figure 8 shows the stress contour from a finite element model emphasizing stress concentrations near the transition from crank pin to web.

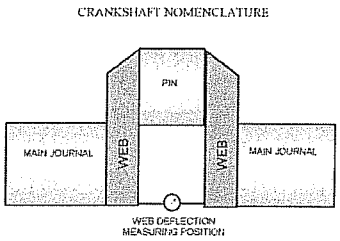

Figure 5. Web Deflection Measurement

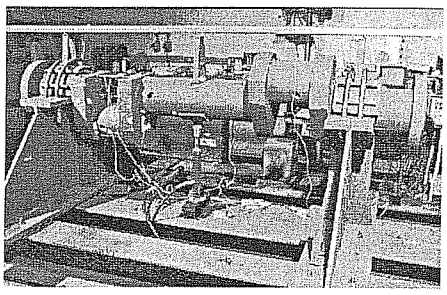

Figure 6. Laboratory Characterization - GMV Crankshaft

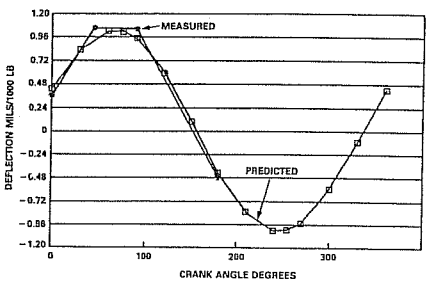

Figure 7. Web Deflection vs. Crank Angle - HBA Shaft

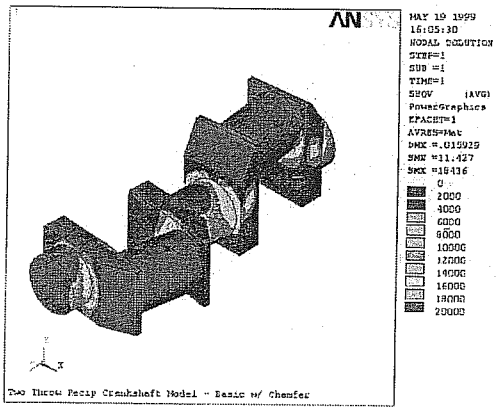

Figure 8. Stress Contours in Bent Crankshaft

3 Thermal Distortion

A compressor installation has sources of heat, including compressor work, bearing friction, power cylinders in integral compressors, and the thermal mass of hot oil in the sump. The hot sump imposes a temperature distribution on the foundation, which tends to distort as a result. Testing has shown this as a transient phenomenon, superimposed on misalignment induced by structural deterioration. It complicates alignment decisions and the precise interpretation of periodic web deflection measurements. Figure 9 shows measurements obtained by a laser system. It compares changes in alignment following a cold start for a compressor on a full bed grout, and an identical compressor, chock mounted, with an air gap under the compressor base[6]. Both traces reveal a tendency to sag in the first 24 hours of the start-up, followed by a gradual reversal of this sagging, as the center of the compressor moves up relative to its ends. The clear variability in magnitude and direction of transient thermal misalignment has put into question an early practice of aligning under cold conditions with an offsetting sag in anticipation of upwards distortion. Many organizations now align level under cold conditions, and assure web deflections are acceptable under "hot conditions". This figure also shows reduced distortion with an air gap under the compressor. Figures 10 and 11 show how the high thermal inertia of a large concrete block causes long time constants in the thermal processes. It illustrates the substantial difference between the temperature distribution predicted one hour after start-up and 48 hours after start-up[7,8]. Figure 11 compares predicted thermal distortion for a full bed grout and chock mounts of both steel and epoxy material. The magnitude of thermal distortion reflects heat transfer to the block. Epoxy chocks maximize insulation both by the air gap and the low conductivity of epoxy material. Steel chocks reflect the air gap benefit, but the steel

represents a significant path for heat flow. The full bed grout allows heat transfer across the entire compressor base, resulting in high distortion.

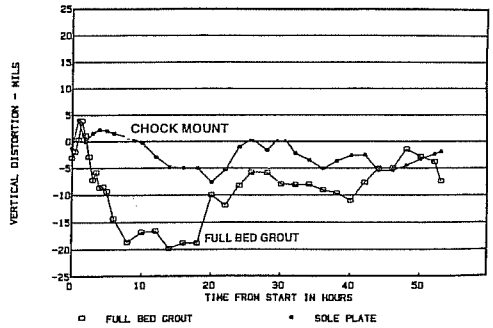

Figure 9. Comparison of Vertical Distortion for Chock Mount and Full Bed Grout Units Over First 53 Hrs. of Test

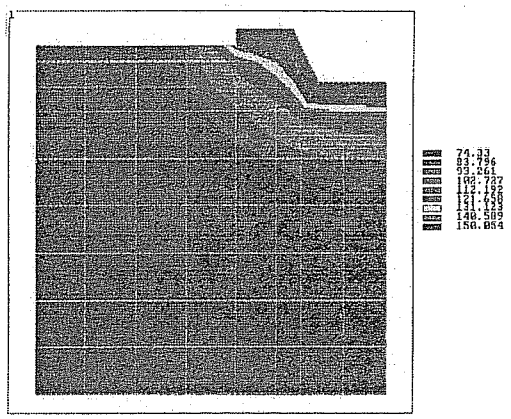

Figure 10a. Transient Temperature Distribution in a Full Bed Mounted Unit at Time = 1 Hour

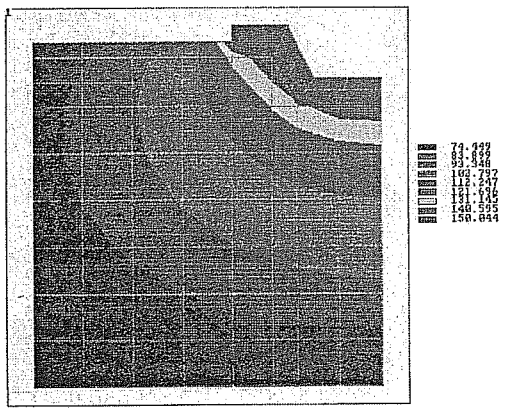

Figure 10b. Transient Temperature Distribution in a Full Bed Mounted Unit at Time = 48 Hours

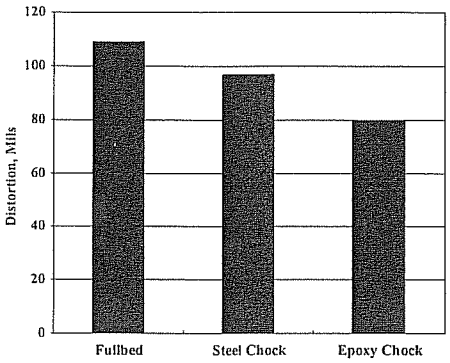

Figure 11. Effect of Compressor Mounting Method on Thermal Distortion Predicted for a 40 Ft. Long Block

4 Compressor Forces

Traditional analysis and design of the mounting system uses the global shaking forces and moments as an input. Early investigations of high compressor vibrations in polyethylene service[9] make clear the total inadequacy of this approach; using the global forces and moments implicitly assumes the compressor frame suffers no bending under the distributed action of these forces. For large compressors, Figure 1, and many other studies[10] have made very clear the frame experiences substantial bending and other significant deflections under both inertia and gas loads.

Figure 12 shows a finite element model of a complete installation used to investigate sensitivity of transmitted force predictions to assumptions about frame flexibility. Figure 13 compares predictions of transmitted force under inertia load for three assumptions: infinitely flexible (soft), infinitely rigid, and most realistic (the finite element predictions). This comparison makes clear that the most realistic assumption gives forces ten times those from the rigid frame assumption. The simple infinitely flexible assumption produces forces about 2.5x the most realistic assumptions[11,12]. Of course analyzing every installation by finite element modelling is costly and probably unnecessary. This recognition has led to a pragmatic, but apparently still conservative approach: calculate all tie-down forces on the basis of local individual cylinder forces (rather than the global forces). This calculation implicitly assumes the frame is totally flexible, so cut the result in half to give some credit for the structural resistance of the frame. For design purposes, the result tends to be manageable and apparently conservative[13].

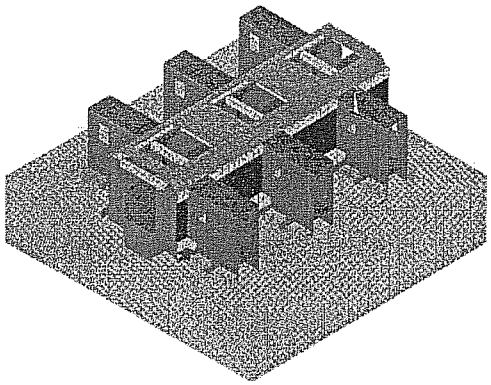

Figure 12. Model of Block and Frame

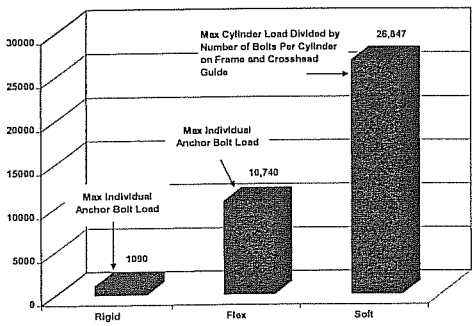

Figure 13. Anchor Bolt Loads for Rigid, Flexible, and Finite Element Analyses

5 Restraining Compressor Forces

For any compressor clamped to a series of flat chock mounts by anchor bolts, friction represents the restraint for horizontal forces. Equation 1 gives the required normal force across the interface:

$$F_n = F_h/\mu \qquad (1)$$

where:

F_n and F_h = normal and horizontal forces.

μ = the coefficient of friction.

Given the preceding way to calculate the horizontal force, Equation 1 requires knowledge of a friction coefficient to calculate the required normal form.

Figure 14 shows the schematic of a test rig used to generate a substantial body of friction data for various interface combinations of cast iron, epoxy, steel, and composite material. Figure 15 presents in bar graph form one of a number of data sets providing both friction coefficient and the standard deviation estimate from multiple tests of multiple samples. Figure 15 covers four conditions (dry breakaway; dry sliding; oily breakaway; and oily sliding). When sliding sets in, the friction restraint drops below the initial breakaway magnitude and the presence of oil seriously derates the coefficient of friction. Reference[14] provides a body of data for different epoxy products and other materials.

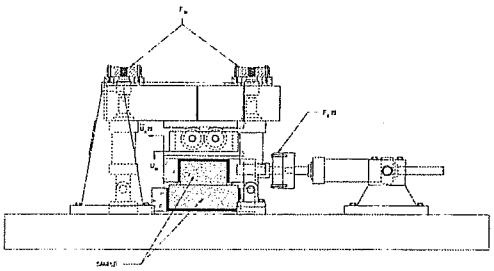

Figure 14. Schematic of Friction Test Rig – Side View

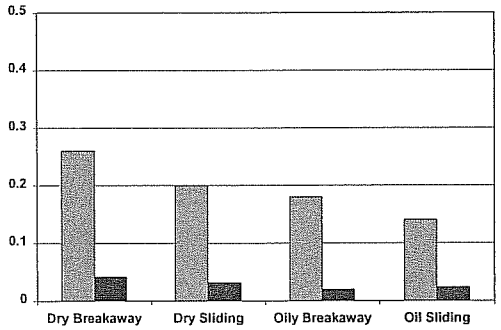

Figure 15. Typical Coefficient of Friction Data for Cast Iron on One of Several Materials Tested

Equation 1 and knowledge of friction enables calculation of the required normal force, which must be designed for and maintained over time. The use of polymeric materials in most grouts and many chocks demands attention to the effects of time. Polymeric material, even under a constant compressive load, deflects by an amount which increases with time and with temperature. This influences the mounting system's ability to maintain tension. A system tensioned when cold heats up rapidly during startup, causing additional compression, which makes it important to retighten at temperature. Even after retightening, any loaded grout material continues to deflect in compression. Figure 16 shows a test fixture used to generate creep data for epoxy materials. This fixture applies an essentially constant load through a soft spring. Strain measured at the center of each specimen, divided by the applied stress, yields the compliance (ratio of strain to stress) under plain stress conditions. Figure 17 shows example compliance data for an epoxy grout material. The creep deflection can be calculated as:

$$\delta(t, T) = J(t, T)\, Fh(F_2/F_1)/A \qquad (2)$$

where:

δ, J, F, h, and A = deflection, compliance, normal force, thickness, and area of application of the force.

F_2 and F_1 are correction factors for nonlinearity and shape, which for a convenient estimate may be assumed equal. Reference[15] provides a basis for calculating F_2 and F_1, and a much larger base of creep data. The references for friction and creep data are available over the Internet.

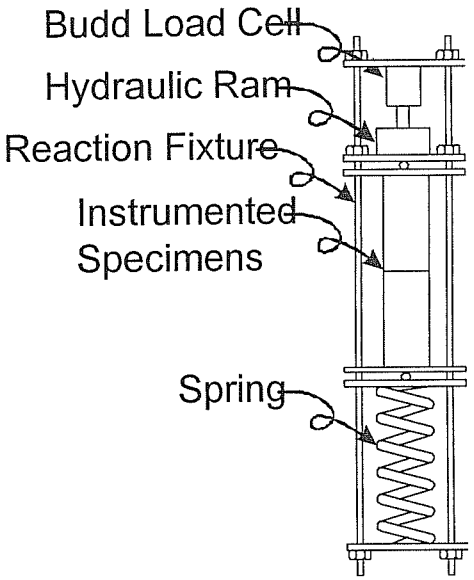

Figure 16. Schematic of Creep Test Fixture

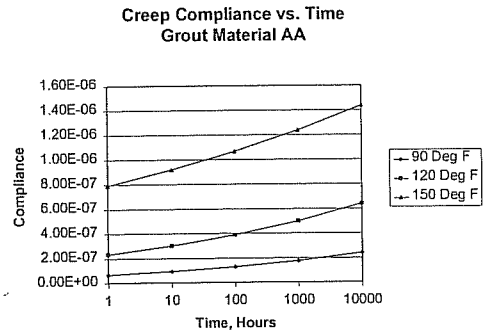

Figure 17. Creep Compliance ($in^2/lb.$) vs. Time; Grout Material AA

6 Anchor Bolts

Anchor bolts create the forces to hold the compressor down. Various factors influence anchor bolt effectiveness (particularly material, length, termination, and diameter). High strength steels[16] greatly improve upon the holding ability of older anchor bolts, and maximize the range of load capacity.

A long anchor bolt (over 4 feet) is beneficial[17], and a growing practice seeks to maximize anchor bolt length by terminating it in the mat below the foundation block! This maximizes creep tolerance. It moves the termination point far from high tensile stress, and sources of oil. It puts the termination, a likely point of cracking, out of sight.

The termination is critical, particularly with the high bolt loads needed to hold the compressor. Figure 18 shows four terminations with undesirable features. The J and L termination can straighten and pull out, and should never be used. A square plate produces high stress points at the corner. A thin washer does not transmit loads effectively. A thick washer or a nut tack welded to the bolt provide the best termination (see Figure 19). Even with the best termination, the concrete experiences high tensile stresses at some point near the termination, and almost inevitably cracks here. The cracking is tolerable provided high rebar density is specified (0.2% to 1% on area), and that all termination are kept well away from the block surface by at least one-third of a meter, and ideally are placed in the mat.

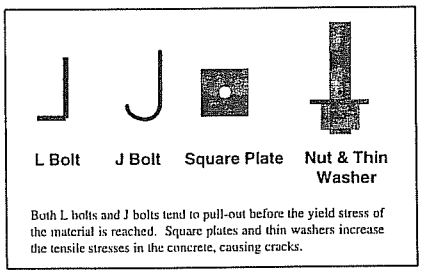

Figure 18. Undesirable Anchor Bolt Terminations

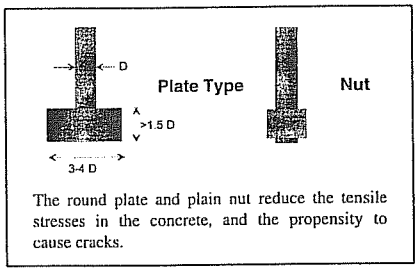

Figure 19. Preferred Anchor Bolt Terminations

Session 4

As Figure 20 shows, bolt terminations too near the block face produce a horizontal crack line in the foundation of a large eight-cylinder process compressor. Figure 20 also shows how vertical interfaces between soleplates and grout and the corners of the pan area can experience cracks. Expansion joints help avoid the interface cracks; avoiding sharp corners and post-tensioning can help control pan area cracks.

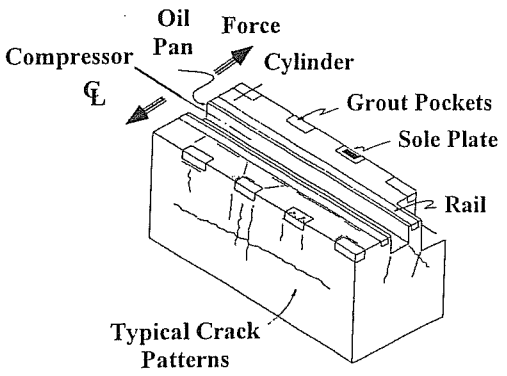

Figure 20. Foundation Block Isometric View – Compressor Area Showing Grout Pocket, Soleplates and Observed Areas of Cracking

A long anchor bolt, well terminated and tensioned to hold friction between maintenance intervals, will greatly help towards a robust compressor installation.

7 Condition Monitoring

Many old compressor installations reflect deterioration from a combination of sustained dynamic loads, inadequate maintenance, and insufficient knowledge in the past to ensure strong mounting and a robust foundation block. The almost universal presence of oil leaks seems to aggravate damage growth, possibly by transporting damaging chemicals, and by generating hydrodynamic forces which accelerate crack growth. A problem facing many operators of large reciprocating compressors is to assess how serious is the deterioration of a particular compressor foundation. At what point does it become prudent to repair the foundation and lower the increasing risks of disruptively failing bearings or crankshaft? Web deflection measurement remains the most widely practiced condition monitoring technique. Research funded by GMRC has built on the work of Bishop and James[18], to develop a Windows software package. It accepts the web deflection data set coupled with the crankshaft and bearing geometry. This package ("Webmap"[19]) presents graphically the deflected shape of the entire crankshaft, as illustrated in Figure 21. Recent extension provides an estimate of stress distribution, which can account for the stress amplifying influence of reverses in sign of misalignment between adjacent bearings, as well as the corkscrew nature of some deflections.

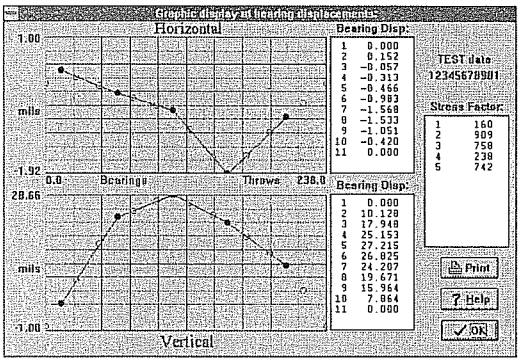

Figure 21. Webmap Output: Crankshaft Deformed Shape, Horizontal and Vertical

Many compressor installations use a simple temperature switch or melt-out device to detect and shut down immediately in the event of excessive bearing temperature, as a safety measure. More recently, an increasingly number of compressor operators have installed thermocouples or RTDs in each main bearing, in order to monitor temperature values. There remains a need to develop robust decision-making practices, which can effectively discriminate sufficiently severe conditions, through main bearing temperature monitoring, to warrant shutdown and maintenance action. Figure 22 shows the variation in temperature following a startup, which led to a bearing failure (Bearing No. 7) within a short period of time. Clearly, this bearing reflected a serious deviation in temperature from other bearings at an early stage even when the absolute temperature had not reached a trip level. Reference[20] shows that more comprehensive use of the multiple temperature channels to detect such deviation at an early stage could protect against consequential damage, which in this example led to crankshaft failure, as well as loss of a bearing.

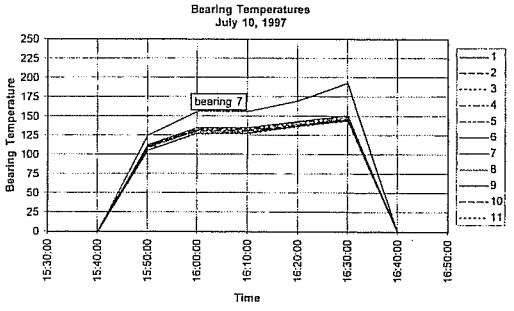

Figure 22. Bearing Temperature During Failure

8 Future Research Plans

Near-term research plans include the following:

- Extended analysis of relationships between crankshaft stress and bearing misalignment.
- Integration of these relationships into the GMRC WEBMAP software.
- Investigation of damage mechanisms implicit in measured compressor frame vibrations.
- Monitoring crankshaft dynamic stress during operation to include start-up, daily temperature changes, and load swings as a complement to static web deflection data.
- Investigation of leaked oil as a damage mechanism: its primary sources, requirements to control it, and the processes by which it aggravates foundation deterioration.

The results of these investigations should further enhance future abilities to install and maintain reliable compressor foundations and mounting systems for the economic life of a reciprocating compressor.

9 Acknowledgements

This paper presents research supported by PRCI, GMRC, and a number of individual companies. The authors wish to acknowledge and thank these organizations for their support and encouragement.

References

[1] Smalley, A. J., "Measurement, Evaluation, and Control of Compressor Alignment," American Gas Association Operating Section Distribution/ Transmission Conference, May 21-24, 1989, New Orleans, Louisiana.

[2] Smalley, A. J., "Crankshaft Protection: Guidelines for Operators of Slow Speed Integral Engine/Compressors," GMRC Technical Report No. TR 97-1, January 1997; www.gmrc.org.

[3] Smalley, A. J. and Pantermuehl, P. J., "Foundation Guidelines," GMRC Technical Report No. TR-97-2, January 1997; www.gmrc.org.

[4] "Crankshaft Failure Survey" (Volumes I and II); SwRI Project 04-6426, April 1995.

[5] Smalley, A. J. and Palazzolo, A. B., "Crankshaft Stress Reduction Through Improved Alignment Practice," 1983 Year-End Report for Project PR15-174, Pipeline Research Committee of the American Gas Association, January 20, 1984.

[6] Smalley, A. J., "Crankshaft Stress Reduction Through Improved Alignment Practice", Project Final Report Incorporating Report on "Field Test of a Sole Plate Mounted Reciprocating Compressor," Year-End Report for Project PR15-174, Pipeline Research Committee of the American Gas Association, December 1985.

[7] Smalley, A. J. and Mandke, J. S., "Analyzing Thermal Distortion of Compressor Foundation Block," *Pipe Line Industry*, June 1994, pp. 21-25.

[8] Mandke, J. S. and Smalley, A. J., "Foundation Thermoelastic Distortion," Pipeline and Compressor Research Council, GMRC Report No. 89-3; www.gmrc.org.

[9] Smalley, A. J., "Dynamic Forces Transmitted by a Compressor to its Foundation," ASME/Internal Combustion Symposium at the 1998 Energy-sources Technology Conference and Exhibition, January 10-14, 1988, New Orleans, Louisiana.

[10] Smalley, A. J. and Pantermuehl, P. J., "Realistically Assessing Load Severity on Concrete Foundations and Mounting Systems for Large Reciprocating Compressors," presented at the 1998 American Concrete Institute Spring Convention, March 22-27, 1998, Houston, Texas.

[11] Smalley, A. J. and Pantermuehl, P. J., Lewis, R. M., and Johnson, E.A., "New Look at Forces Can Help Minimize Foundation Cracking," *Pipe Line & Gas Industry*, February 1998, pp. 45-51.

[12] Smalley, A. J. and Pantermuehl, P. J., Lewis, R. M., and Johnson, E.A., "Design of Reciprocating Compressor Mounting Systems and Foundations for Integrity and Reliability," 1996 PCRC Gas Machinery Conference, September 30-October 2, 1996, Denver, Colorado.

[13] Smalley, A. J. and Harrell, J. P., "Foundation Design," 1997 PCRC Gas Machinery Conference, October 6-8, 1997, Austin, Texas.

[14] Pantermuehl, P. J. and Smalley, A. J., "Friction Tests – Typical Chock Materials and Cast Iron," GMRC Technical Report No. TR-97-3, December 1997; www.gmrc.org.

[15] Smalley, A. J., "Epoxy Chock Material Creep Tests," GMRC Technical Report No. TR 97-5, December 1997; www.gmrc.org.

[16] "Standard Specification for Alloy-Steel and Stainless Steel Bolting Materials for High-Temperature Service," ASTM Designation: A193/A 193M-94b.

[17] Pantermuehl, P. J. and Smalley, A. J., "Compressor Anchor Bolt Design," GMRC Technical Report No. TR 97-6, December 1997; www.gmrc.org.

[18] James, R. W. and Bishop, L. E., Jr., "Calculation of Integral Compressor Misalignments from Measured Web Deflections," Energy Sources Technology Conference and Exhibition, Dallas, Texas, February 15-20, 1987.

[19] Harrell, J., Webmap User's Manual, www.gmrc.org.

[20] Gomez-Leon, S. and Smalley, A. J., "Main Bearing Temperature Monitoring," GMRC Technical Report No. TR 97-7, April 1998; www.gmrc.org.

The Effects of Considering Unsteady Real Gas Flow in a Reciprocating Compressor Plant Model Upon the Accuracy of Performance Prediction

Dr. Dobrivoje Ninkovic
R & D Group
Sulzer-Burckhardt Eng. Works Ltd.
Winterthur, Switzerland

The Recip – A State-of-the-Art Compressor
Nov. 4-5th 1999, Dresden, Germany

Abstract

Presented in the paper is the outline of a mathematical model describing unsteady real gas flow in a reciprocating compressor plant. The model consists of real gas versions of the method of characteristics, the Lax-Wendroff pipe flow algorithm, and a method for treating discrete flow resitances in a generalized manner. The results presented show the effects of shifting the boundary conditions from the cylinder away to their natural locations (plant inlet and outlet) upon the performance prediction accuracy, demonstrate the interactions between the valve and gas dynamics, and the potential for valve function optimization and troubleshooting.

1 Introduction

From the standpoint of a non-specialized reciprocating compressor manufacturer, the res-pective market is characterized by ever changing specifications as regards the compo-sition of the gas mixture to be compressed, the operating conditions, i.e. the pressure and temperature ranges, and the mode of operation (constant vs. variable speed) involved. While satisfying the accuracy of the performance data stipulated by the customer can be achieved on the basis of charts and empirical coefficients in a narrow application range, sophisticated performance prediction methods are needed if high accuracy is to be maintained over a wide range of operating conditions. The latter involve modelling all relevant physical phenomena, augmented by model calibration on the basis of high quality experimental data.

A typical state-of-the-art reciprocating com-pressor sizing model considers heat transfer in the cylinder, leakages, and valve dynamics, and accounts for the real gas behaviour in all model equations. The boundary conditions imposed when integrating the model equations of individual stages consist customarily of constant pressures and temperatures in the respective valve plena. One such model was described by the present author in an earlier paper[1]. While the accuracy of the plant sizing thus obtained is satisfactory in most cases, the decoupling of the cylinder and the valves from the gas dynamics in the neighbouring vessels and pipes gives rise to errors, especially when significant pressure pulsations are present in the later elements. Thus disposing of the cons-tant boundary conditions in favour of unsteady real gas flow in the cylinder attachments can further improve the quality of the performance prediction, and afford the level of detail suitable for valve optimization and diagnostics purposes. Furthermore, accounting for the interaction between valve dynamics and the pressure pulsations is now being stipulated by the Design Approach 3 of API618 Ed. 4 also for the so-called acoustical pressure pulsation prediction methods[2]. In view of these factors it was felt that exploring further possibilities for improving the accuracy of the performance prediction and valve optimization by extending the cylinder model to a comprehensive compressor plant real gas unsteady flow model capable of catering for pipes, pulsation dampers, heat exchangers, and general throttling devices was worth the extra effort.

2 Description of the model

2.1 Previous work

Referring to the simulation of gas flow in reciprocating compressor plants, the first application of modern numerical methods to this problem is due to Benson and Üçer[3]. Practically at the same time, a noteworthy activity was taking place at the University of Strathclyde[4]. The models described in ([3]) and ([4]) were similar in that they both used a second order finite difference scheme to solve for flow variables in the pipework, based on the ideal gas assumption. Unfortunately, the work done in the area of ideal gas compressor flow simulation in those fruitful years did not lead to any publication worth of note from the standpoint of real gas dynamics thereafter, with a possible exception of a hint at the use of real gas parameters in the computation of the pipe gas flow in a Purdue Conference article[5].

Because a reliable cylinder model of ([1]) was already available at the outset of the project phase outlined in this paper, the approach adopted was to find a one-dimensional gas dynamics program capable of catering for real gas flow through typical compressor plant components, and connect it to the cylinder model. However, a market analysis performed to this purpose failed to produce an acceptable program of this kind. Indeed, a general lack of methods for dealing with the relatively "cold" (-180 to +250°C), low Mach number (<0.5) real gas dynamics characterizes the state-of-the-art, as e.g. witnessed by the fact that the oldest technique for calculating one-dimen-sional gas flow, namely the method of charac-teristics, has only comparatively recently been updated to handle real gases[6]. The approach was thereupon changed inasmuch as to find a program capable of good quality simulation of unsteady pipe flow of ideal gas, extend it in order to cater for the real gas effects, and integrate it with the existing real gas cylinder program to obtain the real gas unsteady flow compressor plant simulation program envisaged. Among several alternatives, a proprie-tary program used by several major European IC engine manufacturers was chosen as the basis for this development (hereafter referred to as the kernel). In addition to a proven track record in the area of reciprocating machinery, the program is backed by an extensive expe-rimental data base pertaining to various ele-ments commonly encountered in a pipework, such as various kinds of T-joints, etc., which saves a lot of time and effort.

The kernel differentiates between unsteady gas flow in pipes, and quasi-steady throttling flow at the pipe ends[7]. The throttling device at a pipe end represents a generalized resistance element, and can be as simple as an orifice or as comprehensive as an engine cylinder. A complex system can thus be built up of well-defined basic elements in a systematic manner, using always the same interface to connect the pipes with other components. Adding a new element to the system involves modelling the processes taking place internally, and respecting the interface formalism when connecting the former to the pipes.

2.2 The cylinder model

Although the cylinder model is documented in ([1]), its salient features will be repeated here for the reader's convenience. The model consists of differential equations of mass and energy balance for the gas trapped within the cylinder control volume, closed by a real gas equation of state. The cylinder walls are non-adiabatic; and their temperature is kept constant within a single cycle, but allowed to vary from one cycle to another until steady state is reached. A comprehensive model of the interaction between the valve sealing element dynamics and the real gas flow through the valve passages is also included.

The assumption of constant pressure at the system boundaries stipulated in the original model of ([1]) has now been dispensed with by modelling the suction and delivery valve plena as constant volume, variable gas state vessels, communicating with the neighbourhood by means of the above mentioned generalized throttle and pipe mechanism. The extensive know-how gained in the process of developing the cylinder model has been fully brought to bear on the valve plenum model. This includes heat transfer between the gas and the plenum walls separating it from the coolant and the outside air (or, indeed, an ice cover in the case of low suction temperatures), time-varying, cycle-constant wall temperatures, and a real gas version of the energy balance equation.

The time-dependent governing equations of the composite cylinder model are integrated numerically by a predictor-corrector algorithm within the iterative computation framework of the kernel.

2.3 The pipe flow model

The non-linear, hyperbolic partial differential equations describing the one-dimensional pipe flow are solved in the kernel by means of the well-known Lax-Wendroff two-step algorithm (e.g. [8]). Although CFD has produced several more sophisticated and accurate algorithms since the appearance of the latter, it was decided to retain it in the present project phase for reasons of experience and programming simplicity.

Since the governing equations in their native form are not restricted to a particular fluid model (indeed, the same algorithm is used to simulate water flow), it is only the computa-tional part of the algorithm that has to be modi-fied in order to make it capable of calculating the real gas flow. Even so, the modifications needed are by no means trivial, since the real gas correlations, such as e.g. Lee-Kesler[9], are customarily expressed in terms of pressure and temperature as the independent variables, whereas the pipe flow conservation laws are formulated in terms of the vector $\left(\rho, \rho \cdot w, \rho\left(u + w^2/2\right)\right)$, wherein ρ stands for the gas density, w for the velocity, and u for the internal energy. A direct connection between the two can only be effected by time-consuming iterative computations at each time and space step.

Provided the solution vector does not fluctuate appreciably over a particular pipe segment, one can linearize the gas data correlations around the mean values of pressure and temperature, and thus save a significant amount of compu-tation time. This is the solution adopted in the current version of the real gas Lax-Wendroff pipe flow algorithm.

The pipe model used allows for gradual cross-section variations and wall friction. A simple means is provided for taking into account heat transfer between the gas and pipe wall in that the latter is assumed to have temporally and spatially constant temperature that has to be specified by the user. Strictly speaking, this assumption is valid only over short pipe seg-ments, and it is planned to replace it by a more realistic model in the next project phase.

The pipe flow algorithm needs to be connected to the boundaries in some way; and the additional information needed is usually provided by the method of characteristics[8]. The latter is itself a pipe flow calculation method, set aside in the seventies by the numerical algorithms, such as e.g. Lax-Wendroff.

A full derivation of a real gas version of the method of characteristics has been done by Flatt[6]; it is based on the existence of two distinct, gas state dependent isentropic expo-nents for a real gas, e.g.

$$p \cdot v^{\kappa_{p,v}} = const. \quad \text{and} \quad p \cdot T^{\frac{\kappa_{p,T}}{\kappa_{p,T}-1}} = const.$$

The equations of characteristics thus obtained have the same form as their ideal gas counter-parts; it is the implicit differences in the underlying gas models that produce different results in the ideal and the real gas cases.

2.4 The generalized throttling element

As the gas flows through a typical recipro-cating compressor plant, pressure loss is incur-red at a number of discrete devices, such as valves, orifices, abrupt cross-section changes, T-joints, etc. Since a theoretical treatment of each of these elements is beyond practicality, one resorts to simplified modelling and the use of empirical pressure loss figures. One such figure is the discharge coefficient:

$$C_d = \dot{m}/\dot{m}_{th}$$

which is defined as the ratio of the mass flow rate measured and its theoretical counterpart under the same conditions. The latter corresponds to frictionless isentropic flow from the upstream stagnation conditions:

$$\dot{m}_{th} = A_2 \rho_2 \sqrt{2(h_{01} - h_2)}$$

where the indices 1 and 2 refer to the upstream and downstream conditions, respectively. Knowing the ideal mass flow rate and the discharge coefficient, one is able to arrive at the true flow rate through the device. However, in comparison with the customary ideal gas case, computing the above enthalpy difference in the case of real gases, and in the context of the coupling with the pipe flow, represents a major challenge. Among the problems encountered is the need to solve the inverse problem, i.e. obtaining e.g. a pressure given the mass flow rate, the existence of different isentropic exponents for various state variable pairs (e.g. *p-v*, *p-T*, etc.)[6], and the strong variability of the former over the range of operating conditions of interest. For example, the *p-v* isentropic exponent may easily assume the value of unity, creating thus a singularity in the standard choking criterion equation:

$$\left.\frac{p_2}{p_1}\right|_{crit.} = \left(\frac{2}{\kappa+1}\right)^{\frac{\kappa}{\kappa-1}}$$

Describing the set of formulae arrived at after extensive theoretical and numerical studies lies beyond the scope of the present paper. They have been implemented in the current version of the program, and are at the moment being subjected to extensive testing.

3 Results

Since most of the theory outlined above repre-sents entirely new developments and deriva-tions, the first objective defined for the initial test phase was to check the simulation results for plausibility. This was to be followed by accuracy tests (comparison with measure-ments), and gathering of data on the execution time for the purpose of program optimization. The last point should not be underestimated, for with an integration step of 0.1 Deg. there are at least 7200 calls to the iterative real gas subroutine set pro crankshaft revolution and piston side, without taking into account the need to iterate the mass and energy balance equations.

It should be noted that the current version of the software consists solely of the first imple-mentation of the computational part, i.e. there are no pre- and/or postprocessing routines whatsoever. This makes for a short turnaround time in case an error is found, and restricts the investment to the bare essentials. On the nega-tive side, it certainly does not contribute to the simplicity of data input and results analysis.

The first set of test results to be presented here refers to an ideal gas case, and concentrates thus on the global effects of augmenting a cylinder model by the attachments. The former include the capacity, gas temperature, and indicated power. The discussion proceeds by comparing the predictions obtained with the two model versions to each other and to the data obtained on the test stand. It is an abridged version of the results already presen-ted elsewhere[10]; but since this example shows very clearly the effects mentioned, it was felt unnecessary to create a new one.

The measurements concerned were made in 1982 on a single cylinder, double-acting, lubri-cated machine, compressing nitrogen at vari-ous speeds and pressure ratios. Their purpose was to acquire accurate performance data of the machine in question; and this makes it an excellent object for the study at hand.

With reference to *Table 1* below, the capacity predicted by the model outlined in ([1]), i.e. constant pressure in the valve plena, no pipe-work (referred to as CYL hereafter), and that of a compressor model with attachments (CYL++) is compared to the measured data. Including the cylinder neighbourhood into the simulation clearly corrects the dependence of the capacity error upon the speed displayed by the CYL in this case. The same trend towards reducing the prediction error is observed in the indicated power computed by the CYL++ mo-del (*Table 2*). As to the discharge temperature, both models have a general tendency towards somewhat higher values, which indicates that further refinement of the cylinder and/or valve plena heat transfer models may be required[10].

Table 1
The capacity prediction error (ideal gas)

Speed [rpm]	CYL	CYL++
627	-7.81	-2.24
950	-0.33	+2.27
1500	+9.33	+2.50

Table 2
The power prediction error (ideal gas)

Speed [rpm]	CYL	CYL++
627	-3.74	+1.10
950	-4.41	+1.67
1500	-4.08	-0.79

Referring to *Fig. 1* below, the plots show the traces of cylinder pressure and valve lift against crank angle computed by the CYL model at 627 rpm. Due to a mismatch between the valves and the operating conditions, there is a bad valve flutter, making this case a real challenge to simulate accurately. The valve lift traces computed display a tendency of both the suction and the discharge valves towards early closure when operating against a constant plenum pressure (second plot from the top).

The interaction between the gas and valve dynamics brought about by the inclusion of the valve plena and the associated piping in the new

model modifies the flutter frequency of both valves (*Fig. 2*, bottom traces), making them close almost on time, i.e. very near to the respective piston dead centres. This improves the cylinder performance, giving rise to the higher delivery rates at 627 and 950 rpm in the case of CYL++, and bringing the very opti-mistic capacity prediction of CYL at 1500 rpm in line with the data (see also *Table 1*).

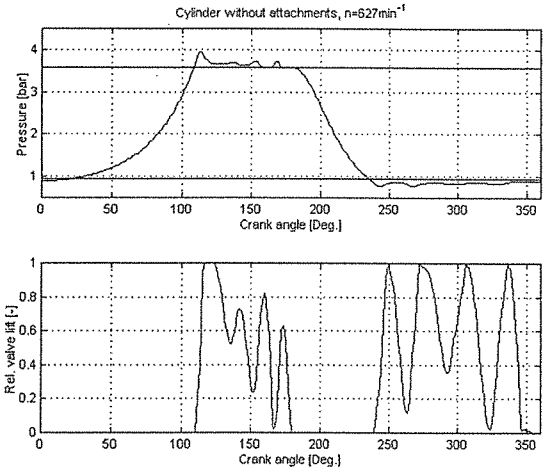

Fig. 1: Cylinder without attachments

The second case study to be presented here concerns a two cylinder, single stage, dry-run-ning ethylene compressor driven by a variable-frequency asynchronous motor drive in the speed range from 320 to 490 rpm. Extensive measurements have been performed in this plant (at customer's site, and under normal operating conditions, i.e. with the compressor feeding the plant), including pressure indi-cation at several speeds on all four piston sides

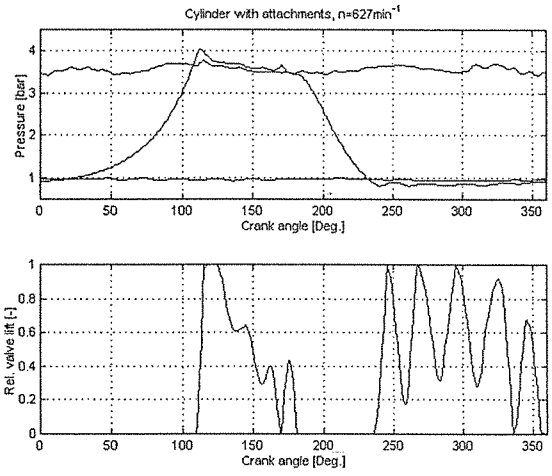

Fig. 2: Cylinder with attachments

of its two double-acting cylinders. This allows not only for making relative comparisons (i.e. between the two models), but - more signi-ficantly - makes it possible to judge the abso-lute accuracy of the predictions by checking for their agreement with the experimental data.

Table 3
Gas parameters for the ethylene plant

Parameter	Suction (50 bar, 60°C)	Delivery (70 bar, 80°C)
Z	0.783	0.757
$\kappa_{p,v}$	1.17	1.19
$\kappa_{p,T}$	1.27	1.26
c_p/c_v	1.59	1.63

Concerning the gas model applicable in the pressure and temperature ranges the plant operates in, this is definitely a real gas case. Referring to Table 3 above, one notes that the compressibility factor *Z* of the gas mixture in question is different from unity, and that the two isentropic exponents have different values. The ideal gas isentropic exponent (last row in *Table 3*) suggests even a value that would be normal for a monatomic gas.

Arguably, this case is not as extreme as, say, the end stage of a hypercompressor feeding an LDPE plant, with a typical delivery pressure of up to 3000 bar. However, the program is also capable of coping with such applications, as has already been demonstrated[10]. It is the exis-tence of good quality experimental data pertai-ning to real gas flow that makes this particular case so interesting.

Referring to *Fig. 3* below, the upper plot shows the cylinder pressure trace computed by the CYL model at the machine speed of 495 rpm, operating at the respective mean values of the suction and delivery pressure measured. While this plot shows nothing extraordinary, the lower one, showing the predicted valve lift traces, reveals a tendency of both valves towards early closure, which may indicate that

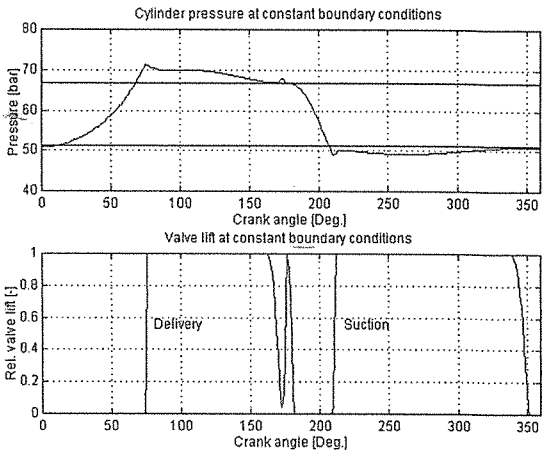

Fig. 3: Real gas case, cyl. without attachments

the springing applied is too stiff for the given application. Indeed, the predicted suction valve closure is at 350°, which reduces the amount of gas entering the cylinder, and hence the efficiency.

Comparing the indicator diagram computed by the CYL model with the measured one (Fig. 4), one notices the disagreement in both the suction and the delivery phase of the cycle, which results in the predicted indicated power being lower than the real one. Although at the first glance one may be lead to the conclusion that the lower indicated power in *Fig. 4* is due to lower valve losses, it should be borne in mind that automatic compressor valves are held open by the pressure difference; thus the predicted position of the pressure traces in the suction and discharge phases is merely the consequence of the constant pressures in the suction and discharge valve plena. In conclu-sion, although in the present case the predicted value of the indicated power is somewhat low, it is not due to an underprediction of valve los-ses. Note that by virtue of the low pressure ratio in the present case, valve losses represent a significant part of the total indicated power (approx. 15%).

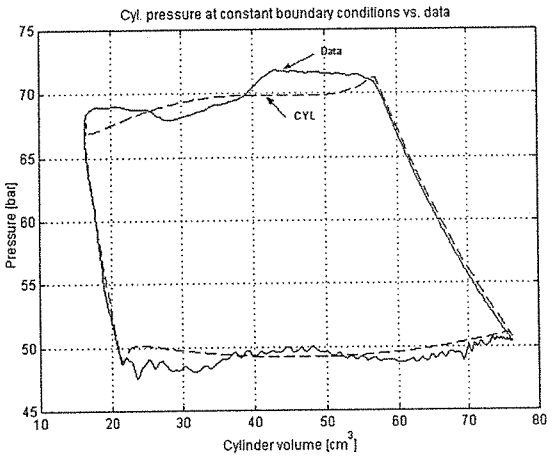

Fig. 4: Real gas case, cyl. without attachments

Simulating now the main part of this plant by means of the CYL++ model (both double-acting cylinders, 25 pipe segments (total length approx. 22 metres), three vessels, and 15 discrete flow resistances) results in the pres-sure traces and valve lift curves shown in the upper and lower plots, resp., of *Fig. 5*. The apparent tendency of the delivery valve towards double closure displayed by the CYL model results has now been replaced by a fully normal valve function; and the early closure of the suction valve predicted previously has now effectively turned into the opposite, being late by some five degrees and showing a tendency towards double closure. Obviously, the chan-ged valve behaviour is the consequence of the coupling between the valve and gas dynamics in both the cylinder and the valve plena.

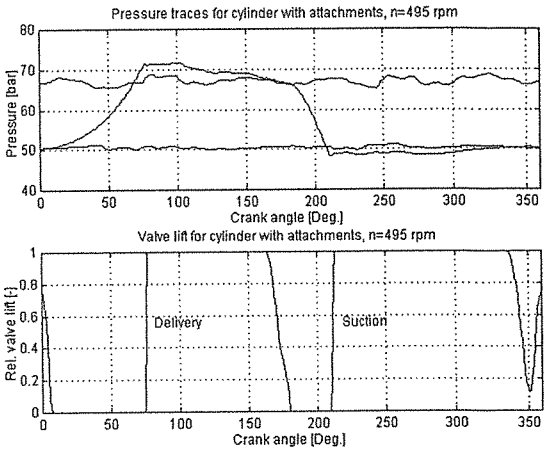

Fig. 5: Real gas case, full plant model

Turning now to the global plant results, the values presented in *Table 4* display the same trend towards higher power and higher end temperature when switching from the bare cylinder model to the full plant model. The fact that the cylinders now work against variable- pressure boundaries results in a higher power expenditure.

Incidentally, the temperatures measured in the valve plena of the two cylinders by the plant control system at the time of data acquistion were 84.1 and 83.7°C, resp. Obviously, the end temperature calculated by the CYL++ model is in a very good agreement with these data.

Table 4
The ethylene prediction results at 495 rpm

Variable	CYL	CYL++
Capacity	42140 kg/h	41580 kg/h
Power	292 kW	308 kW
Temperature	81.5°C	83.6°C

Referring to *Fig. 6* below, the indicator diagram computed by the full plant model shows a much better agreement with the data as was the case in *Fig. 4*. The slight deviations in the suction and delivery phases are most likely due to imperfections in the valve dynamics model and/or its interaction with the gas flow, and merit further investigations.

Concerning the pressure pulsation visible in the suction part of the measured indicator diagram, it is most likely a phenomenon local to the cylinder. As we shall later see, no such pulsation is visible in the pressure signal acquired in the adjoining valve plenum; and the fact that it ceases as soon as the suction valve closes points to a possible flow-induced pulsation downstream of the valve, in the vicinity of the pressure measurement tap (all cylinder pressure measurements were made with transducers installed into the suction valve mounting studs). It also does not seem to be the phenomenon of acoustic pulsations in the cylinder,

taking place between the suction and delivery valves installed opposite to each other, observed experimentally a long time ago also by this company, and treated theoretically by Böswirth[11]. The latter is observed to start

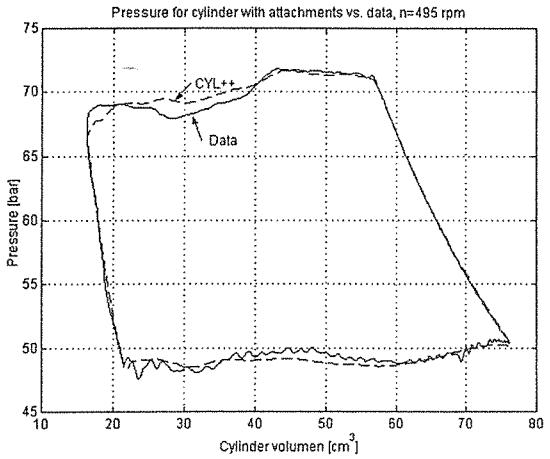

Fig. 6: Prediction vs. data, full plant model

immediately after the delivery valve closes, continuing along the back expansion portion of the cycle until being quenched by the inrush of fresh gas following the suction valve opening.

Presented in *Fig. 7* below is a comparison of the unsteady pressure variation in the suction valve plenum computed by the model (broken line), with the data measured by a transducer mounted in the respective valve cover. While being of similar shape to the measured wave-form, the predicted pressure pulsation is apparently somewhat faster than the former, which is due to the modelling philosophy applied, i.e. the way the actual compressor geometry is broken down into fundamental building blocks, such as pipes, vessels, etc. This sort of disagreement can be dealt with by studying the effects of various geometrical parameters upon the predictions, establishing thus an optimal modelling approach for a given compressor class. However, high quality experimental data of the kind presented in this report are required for such an operation.

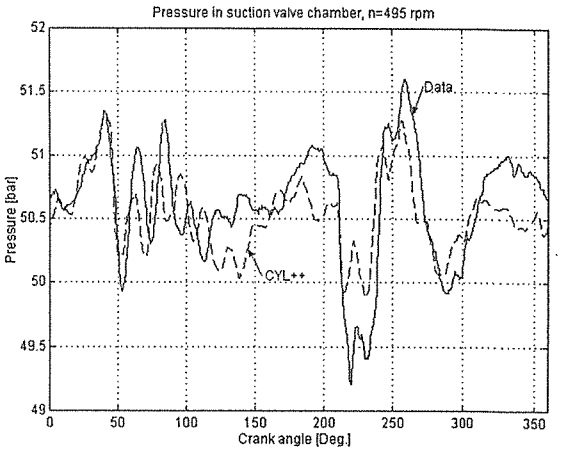

Fig. 7: Prediction vs. data, full plant model

Much better agreement between the predic-tions and the data was obtained in the valve plenum on the delivery side of the compressor (*Fig. 8*). Apart from generally small diffe-rences between the two waveforms, the only component entirely missing in the prediction is the high frequency pulsation clearly visible in the data. This one was observed only in the valve plenum on the cylinder cover side, repre-senting apparently a local acoustic pheno-menon not accounted for by the current valve plenum model. Referring to *Fig. 9*, the respective resonance frequency stands out very

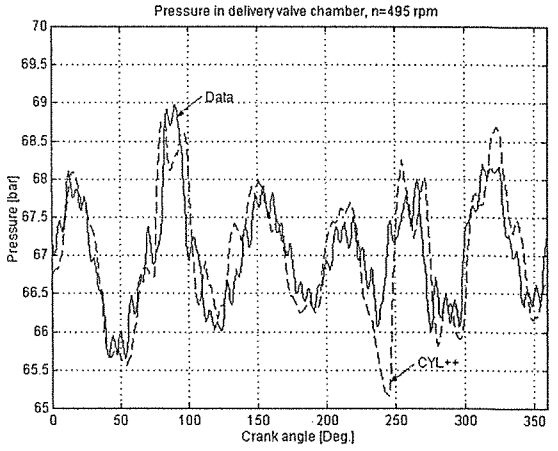

Fig. 8: Prediction vs. data, full plant model

clearly at 454 Hz (55th harmonic of the machi-ne speed). The spectrum of the pulsations measured in the valve plenum on the crank- shaft side of the cylinder (see *Fig. 10*) shows a weak resonance at approx. 425 Hz, which is obviously unrelated to the former one.

From the standpoint of gas dynamics, valve plena are complex structures, their acoustic response being located somewhere between the extremes of a pipe segment, and a pure gas volume (vessel). Representing them as vessels in the present model incurrs the loss of a pipe-like acoustic phenomenon

evident in the data; but the prize won is a good agreement with the data regarding the lower part of the frequency response. Also, no great loss is sustained in not

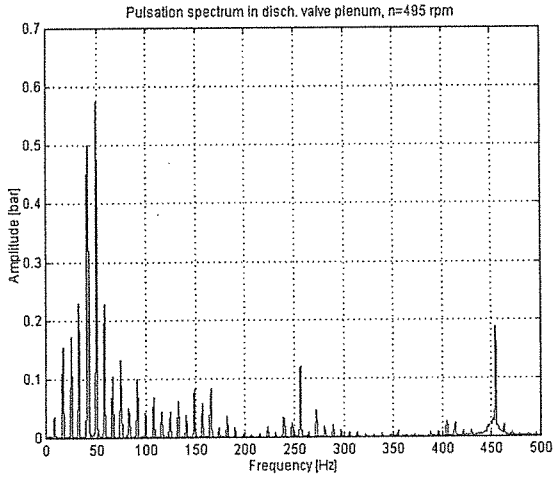

Fig. 9: Measured pressure pulsation spectrum

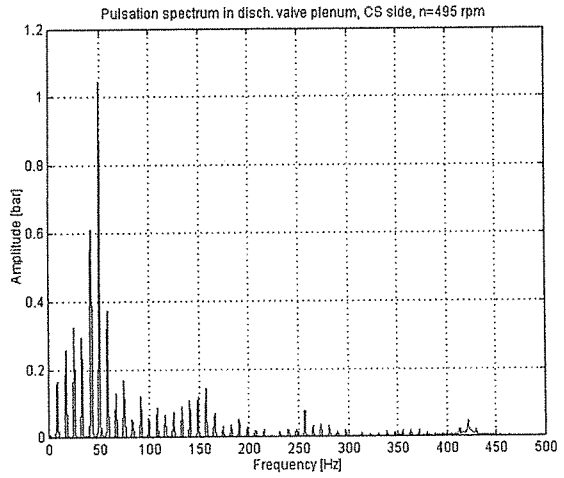

Fig. 10: Measured pressure pulsation spectrum

being able to simulate this high frequency pulsation, for the only element that could theoretically be affected by the aforementioned resonance is the discharge valve. However, typical mechanical natural frequencies of the plate valves used for this compressor size are lower than the observed acoustic resonance by a factor of four to five; thus no interference can occur, and there are no repercussions upon the accuracy of performance prediction. Again, measurements and experience accumulated on a large number of compressors help point the way towards the model required; and it may turn out that a custom valve plenum model is the optimal solution for all cases.

Having an accurate model of the interaction between the valve and gas dynamics may prove to be of paramount importance for the on-line monitoring and valve function diag-nostics; for measuring the sealing element motion is an expensive and time-consuming undertaking even on the test stand. The indi-cator diagram is already a rich source of infor-mation about the cylinder state (e.g.[12]); but being able to conclude as to the valve function on the basis of auxilliary measurements, such as pressure and vibration patterns, would add a dynamic component to it and thus greatly sim-plify valve function troubleshooting.

4 Conclusions

A novel reciprocating compressor performance prediction model has been presented, capable of simulating not only the cylinder proper, but also unsteady flow of real gas in the valve chambers and the associated piping. The interim results obtained so far suggest that the prediction accuracy has benefited from the model extensions, in that the tendency of an earlier model that assumed constant pressure at the cylinder boundaries towards too optimistic results (higher capacity and lower indicated power) has been corrected. The capability of the program to account for the interaction between the valve function and real gas dynamics in the adjacent compressor elements has been demonstrated, providing new pos-sibilities for valve optimization under more realistic conditions.

Work is now proceeding towards gathering high quality dynamic data on the test stand and in customer's plants, aimed at perfecting and/or calibrating various component models (e.g. valve dynamics), and arriving at an optimal plant modelling strategy.

5 Acknowledgements

The author is grateful to the management of Sulzer-Burckhardt Eng. Works Ltd. for the opportunity to realize this project, and the permission to publish the results obtained. This project is a result of a teamwork with Dr. H.-J. Linnhoff and Dr. P. Schindler, both of Ing.-Büro Linnhoff, Bochum, Germany, whose programming contributions and many stimu-lating remarks regarding the theoretical deriva-tions are hereby thankfully acknowledged.

6 References

[1] Ninkovi , D. Performance Prediction of Reciprocating Compressors Working With Real Gas Mixtures Over a Wide Range of Operating Conditions. Proc. 6th European Congress on Fluid Machinery for the Oil, Petrochemical, and Related Industries, The Hague, 1996, pp. 169-177.

[2] Reciprocating Compressors for Petroleum, Chemical, and Gas Industry Services. API Standard 618, 4th Edition, June 1995.

[3] Benson, R.S. and Üçer, A. . A Theoretical and Experimental Investigation of a Gas Dynamic Model for a Single Stage Reciprocating Compressor With Intake and Delivery Pipe Systems. J. Mech. Eng. Sci. 1972 (14), No. 4, pp. 264-279.

[4] MacLaren, J.F.T. et al. A Comparison of Numerical Solutions of the Unsteady Flow Equations Applied to Reciprocating Compressor Systems. J. Mech. Eng. Sci. 1975 (17), No. 5, pp. 271-279.

[5] Perevozchikov, M.M. and Chrustalyov, B.S. Theoretical and Experimental Researches of Unsteady Gas Flow in the Pipeline of the Reciprocating Compressor. Proc. 1994 Purdue Int. Comp. Eng. Conf., pp. 515-520.

[6] Flatt, R. On the Application of the Numerical Methods of Fluid Mechanics to the Dynamics of Real Gases (in German, orig. "Zur Anwendung numerischer Verfahren der Strömungslehre in der Realgasdynamik"). Forschung Ing.-Wesen, 1985 (51), pp. 41-51.

[7] Görg, K.A. Computation of Unsteady Flow in the Pipework of IC Engines Under Special Consideration of Multiple T-Junctions (in German, orig. "Berechnung instationärer Strömungsvorgänge in Rohrleitungen an Verbrennungsmotoren unter besonderer Berücksichtigung der Mehrfachverzweigung"). Ph.D. Thesis, Ruhr-Univ., Bochum, 1982.

[8] Laney, C.B. Computational Gasdynamics. Cambridge Univ. Press, 1998.

[9] Lee, B.I. and Kesler, M.G. A Generalized Thermodynamic Correlation Based on Three-Parameter Corresponding States, AIChE J., 1975, 21, No. 3, pp.510-527.

[10] Ninkovic, D. Improving the Accuracy of Reciprocating Compressor Performance Prediction by Considering Real Gas Flow in the Valve Chambers and Associated Piping. Proc. 7th European Congress on Fluid Machinery for the Oil, Petrochemical, and Related Industries, The Hague, 1999, pp. 177-186.

[11] Böswirth, L. Gas Flow and Valve Plate Dynamics in Compressor Valves, 2nd Ext. Ed. (in German, orig. "Strömung und Ventilplattenbewegung in Kolbenverdichterventilen"), Published by the Author, Vienna, 1998.

[12] Smalley, A.J. et al. U.S. Patent No. 5,471,400.

Free Floating Piston™: A technology to Prevent Rider Ring Wear

by:

Ir. René Schutte

Thomassen Compression Systems BV

Rheden

The Netherlands

The Recip - a State of the Art Compressor
4. – 5. November 1999, Dresden

Abstract:

Changing process and environmental requirements for large horizontally opposed cylinder compressors are dictating the increasing use of non-lubricated cylinders. Improving the sometimes unpredictable life of piston wear bands remains an elusive goal.

Thomassen, having the wish to achieve a consistent and substantial improvement in rider ring life, has taken a radical approach to attempt to solve this problem.

A feasibility and design study indicated that a gas bearing could offer the required properties. A calculation model was developed. Actual pistons were tested statically, and dynamically in a full size heavy duty test compressor. 2000 hours of operation revealed only traces of bedding-in wear on the rider rings. Finally a hydrogen compressor at the DSM site in the Netherlands has been equipped with the FFP™ technology, which is in full time continuous operation for almost a year and a half without rider ring wear. Normally every half year service was required for this compressor.

The Free Floating Piston technology may be used in almost all applications, with all types of process gases, with virtually no wear of wear bands. It may be easily retrofitted to existing machines by virtue of a self contained design.

1 Introduction

Thomassen Compression Systems has designed and manufactured horizontal balanced opposed reciprocating compressors since 1906.

A reciprocating compressor often is a critical component in a production plant. Shutdown of the compressor directly leads to high production losses if a spare compressor is not available. Often plants are equipped with one operational and one spare compressor to prevent high production losses in case of emergencies. High compressor availability and reliability rates are therefore required.

Horizontally opposed reciprocating compressors require regular maintenance, especially with non-lubricated cylinders. However, oil free compressors are to be preferred over lubricated ones. Gas or valve pollution by oil is eliminated. Further, changing process and environmental requirements favour use of non-lubricated cylinders.

Maintenance for non-lubricated compressors may have a greater scope than lubricated compressors due to the unpredictable wear rate of rider rings. Lifetime improvement by material research only remains an elusive goal. Thomassen, having the wish to achieve a consistent and substantial improvement in wear band life, has taken a radical approach to attempt to solve this problem.

This paper describes the process and results of an intensive research and development program carried out by Thomassen, leading to the Free Floating Piston™ (FFP™) design. A summary of the gas bearing technology will be given. Next to this, the results of more than 9000 hours running experience of the FFP™ in a hydrogen production compressor at the DSM site in the Netherlands with virtually no rider ring wear will be discussed.

2 Research path

2.1 Feasibility study

Some years ago Thomassen started a feasibility study to obtain design principles to solve the problem of unpredictable rider ring wear. The contact between rider rings and cylinder liner is a tribological phenomenon. As a result of the contact, wear occurs. The level and unpredictability thereof depends highly on the existence of oil between the two counterparts. The phenomenon may generally be seen as a sliding bearing.

Two options for sliding bearings were considered feasible in a reciprocating compressor. A gas bearing proved to be more attractive than a magnetic one when compared to design requirements.

The principal design requirement is elimination of unpredictable rider ring wear. Other design requirements are incorporation of emergency running properties, feasibility to refurbish existing compressors and high reliability.

A calculation method to determine the properties of a gas bearing under conditions in a reciprocating compressor was not available. Thomassen developed a method to be able to calculate the FFP™ design for any compressor.

2.2 Gas bearing technology

More than a century ago the principles of gas bearing were formulated. Kingsbury then wrote a publication on externally pressurised bearings, describing a method to separate two surfaces by means of pressurised gas. Non were made at that time due to lack of accurate manufacturing facilities.

Gas bearings may be divided into two categories, aerodynamic and aerostatic. In aerodynamic bearings the surface shape in combination with a velocity difference generates a gas film between the two surfaces. Load capacity of an aerostatic bearing follows from an external pressurised gas supply in combination with the surface area. The aerostatic gas bearing principle is used for the Free Floating Piston™ design.

A pressure difference between the gas supply and the bearing environment causes a gas flow and a pressure distribution. The pressure carries the load on the bearing, the flow determining the film between the surfaces. Since a certain pressure distribution is only capable of carrying one specific load, stiffness is introduced to be able to compensate for changes in load. Flow resistance nozzles may be integrated to ensure this necessary characteristic.

3 Free Floating Piston™

3.1 Free Floating Piston™ technology

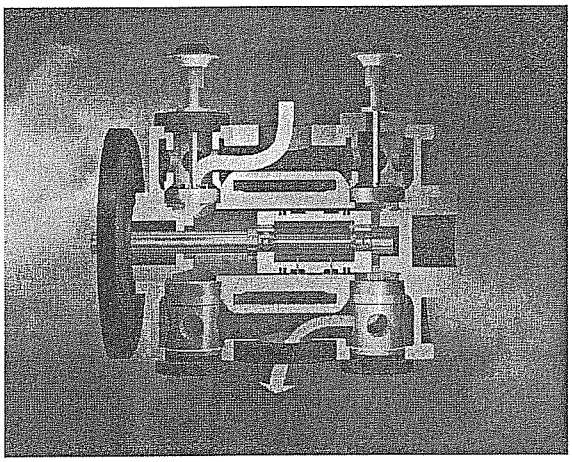

Picture. 1: Free Floating Piston™ technology

The implementation of the gas bearing technology in a piston of a reciprocating compressor involves some changes of the piston design. Compared to Thomassen's original piston design, the rider rings and piston rings have exchanged place. Since pressure drops from discharge level to suction level over the piston rings, a nearly constant pressure exists in-between the piston rings. The constant pressure level fulfils the requirement for a stable gas bearing characteristic. Further small compressor poppet valves have been integrated in the piston faces, enabling gas at discharge pressure to enter the piston during the compression stroke. The gas inside the piston is maintained at a constant pressure. Since a double acting compressor may be used single acting, both piston faces are equipped with the poppet valves to ensure a constant gas supply.

Flow nozzles have been integrated in the rider rings enabling the gas to flow out of the piston. The resulting pressure between piston and cylinder lifts the piston free from the cylinder wall. Spent gas, which is small compared to piston ring blow-by, also escapes as blow-by.

The Free Floating Piston™ design is patented in a number of countries around the world.

3.2 Testing facilities

3.2.1 Static test

After the calculation model was developed, a full scale static test rig was built for two main reasons. First, tests for gas bearings with dimensions at hand had to our knowledge never been performed before. Scaling up of known results would not be satisfactory. Next to this, pressure distributions under various loads had to be measured to be able to verify the calculation model.

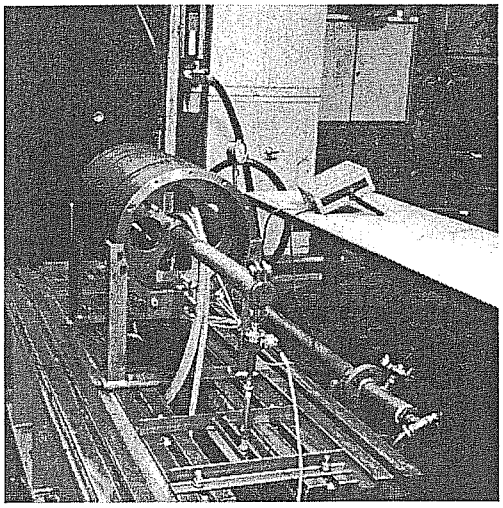

Picture. 2: Static test rig

3.2.2 Dynamic test

After the design had been successfully subjected to test series on the static test rig, Thomassen's heavy duty test compressor was equipped with Free Floating Piston™ technology. The test set-up, with the compressor valves installed, was at first run with an external air supply, to give the opportunity to compare results to these obtained with the static test rig. Subsequently, test operation was with piston pressurisation valves installed

The Free Floating Piston™ functioned as calculated. After a test period of 2000 hours with more than 150 starts and stops, the rider ring showed no wear. Normally the replacement interval was 3000 hours on untreated air. Now, next to imbedded particles and running in scratches, original machining tracks were still clearly visible.

5 Field application

5.1 Introduction

As the development of the Free Floating Piston™ technology was very successful, a duration test in the field was prepared. Since air is not a general medium to be compressed in a production plant, the calculation model was expanded for all kinds of gases. It became possible to install Free Floating Piston™ in a hydrogen compressor at DSM Hydrocarbons production site in the Netherlands. A co-operation was formed, and project sponsoring

was obtained from the Dutch Ministry of Economic Affairs.

This compressor was very suitable for implementation of FFP™ design and was a logical step in the development program. The cylinder dimensions were in the same range as test FFP™'s. Hence, a comparison between the tests performed at Thomassen and the test program at DSM was possible. The process gas is rich hydrogen, suitable to test the extension of the calculation model. The process has two compressors, one operational and one spare. Thomassen was therefore in the position to perform inspections to the compressor equipped with FFP™ at all times.

5.2 Design

First step in the design of Free Floating Piston™ for the DSM compressor was the extension of the calculation program to any process gas. Based on existing theory and tests performed, this extension was completed.

The DSM hydrogen compressor FFP™ design was executed in accordance with FFP™ design requirements.

5.3 Monitoring

The tests to be performed at DSM were planned for one year. During this year the compressor would run continuously. As information to analyse the performance of Free Floating Piston™ was necessary, the compressor was equipped with a Thomassen TCSM-2600 monitoring system. Measurements taken were rod drop as FFP™ monitor, impact and temperatures at valves and stuffing box.

The system was extended with an on-line pressure / volume measurement and a personal computer. A direct telephone line was connected from the computer to Thomassen, so Thomassen was in the position to evaluate the performance of the compressor at all times. An additional measurement to analyse the performance of FFP™ was a pressure measurement in the middle of the cylinder. Several of the calculated properties could be verified with this measurement.

5.4 Test results

At start-up of the compressor a lower noise level was noticed. This was attributed to FFP™ design.

During the one-year test period data was stored at regular intervals after start of service. As an example, data of about one month are shown in pictures 3 to 5. The beginning of the trace is at start-up of the compressor.

For various process reasons, the compressor has been stopped several times during the one-year test. An example is shown in pictures 3 to 5 where the two peaks represent two short stops.

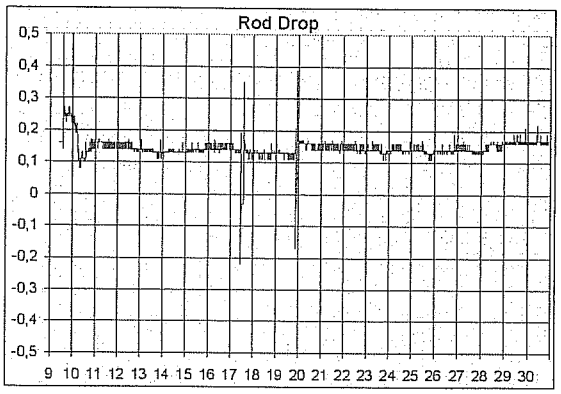

Picture. 3: Measured data from TCSM-2600: Rod drop (time [days] vs. distance [mm])

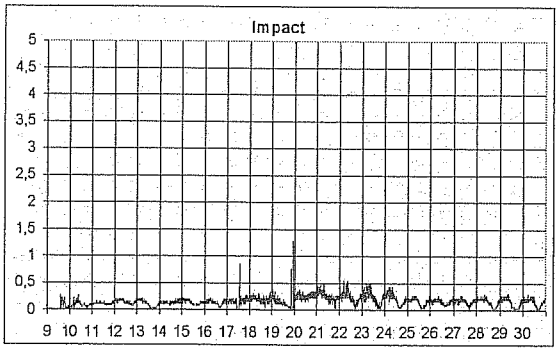

Picture. 4: Measured data from TCSM-2600: Impact (time [days] vs. level [g])

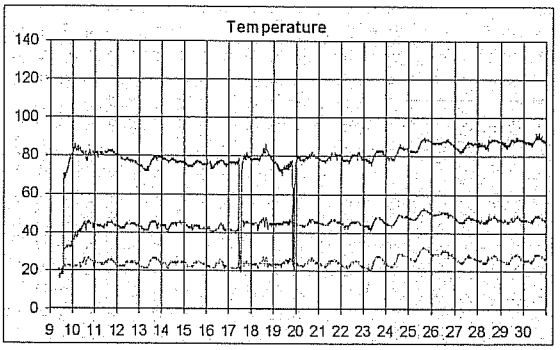

Picture. 5: Measured data from TCSM-2600: from top to down Stuffing box, discharge and suction temperature (time [days] vs. level [°C])

The pictures alone do not reveal all necessary information about the performance of FFP™. Process data has also been analysed regularly to be able to draw conclusions of the measured data. Combined compressor data indicate the progress of

a very stable test period. Rod drop, being a monitor for the performance of FFP™ shows a steady line with only marginal changes due to process changes.

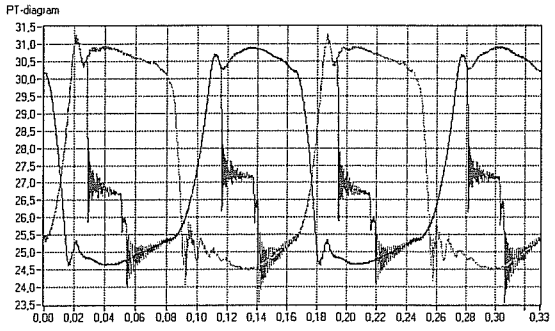

Picture. 6: PT diagram

Picture 6 shows a pressure versus time measurement of the cylinder with FFP™ installed. The picture has been steady over the test period, with only minor changes due to process changes. Power consumption of the test was not affected negatively as was the compressor flow as the design of Free Floating Piston™ compensated for this

Due to the successful progress of the test period, which had been continuously monitored, the scheduled stop after 4000 running hours was postponed. After more than 9000 hours, the compressor was finally stopped for inspection. Where normally piston and rider rings had to be replaced after one year of continuous operation, inspection showed that FFP™ rider rings had the same thickness as original, and piston ring thickness was reduced by a few tenths of a millimetre only. Even several starts and stops did not influence the wear and the behaviour of FFP™ design. Running in or bedded-in particles caused the only wear found on the rider rings.

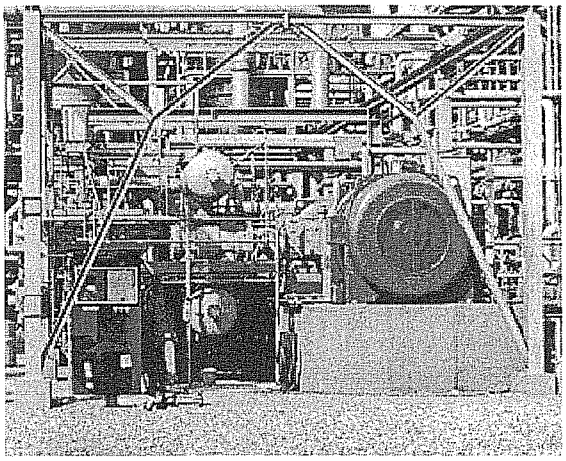

Picture. 6: FFP™ equipped hydrogen compressor at DSM Hydrocarbons site

In comparison to the tests performed on Thomassen's test compressor, the behaviour of Free Floating Piston™ technique has been similar. The adjustment of the calculation model for FFP™ has proven to be correct. Absence of wear found on both compressors was very similar, while process gas properties were very different.

6 Conclusion

Free Floating Piston™ design meets the required operational properties for today, and it is expected, running times of three years for non-lubricated reciprocating compressors.

Wear of rider rings is zero and piston rings is reduced to extremely low values values. Changing existing compressors from lubricated to non-lubricated duty to avoid oil in the process gas with high reliability and availability is now feasible. Moreover, problems caused by oil, such as pollution of valves and associated short valve life, can be solved quite simply. Obvious is the opportunity to solve rider ring problems with non-lubricated compressors.

Free Floating Piston™ design is not sensitive to foreign particles in the process gas. No negative effects were introduced to compressor power consumption and flow. In fact, even a slight improvement was achieved. The lower noise emission of the compressor is the first noticeable effect of the Free Floating Piston™.

The revolutionary Free Floating Piston™ design gives the opportunity to decrease maintenance costs. As lifetime of wearing parts is increased, less stops, scheduled as well as unscheduled are necessary.